

Tactile Sensing with Optical Mouse Sensor

WANG Xin

Supervisor: *Professor* Katsunori SHIDA

A thesis submitted for the degree of *Doctor of Philosophy*

Department of Advanced Systems Control Engineering

Graduate School of Science and Engineering

Saga University

Japan

September 2008

Contents

| | | |
|----------|--|-----------|
| 1 | Introduction | 1 |
| 1.1 | Optical Mouse | 1 |
| 1.1.1 | The Birth of the Computer Mouse | 2 |
| 1.2 | Optical Mouse Sensor | 5 |
| 1.2.1 | Inside An Optical Mouse | 5 |
| 1.2.2 | The Basics of Optical Navigation | 7 |
| 1.2.3 | Advantages of Optical Technology | 8 |
| 1.3 | Optical Position Sensor | 8 |
| 1.4 | Application of Optical Mouse Sensor | 9 |
| 1.5 | Our Work | 16 |
| 2 | Technical Introduction | 19 |
| 2.1 | Robot Arm | 19 |
| 2.2 | MATLAB and Pointer Tracking | 19 |
| 3 | Surface Shape Analyzing Device Using Optical Mouse Sen- | |
| | sor | 23 |
| 3.1 | Introduction | 23 |

| | | |
|----------|--|-----------|
| 3.2 | Sandpaper | 24 |
| 3.2.1 | Grit Sizes | 24 |
| 3.3 | Device Structure | 25 |
| 3.4 | Experiments | 28 |
| 3.5 | Conclusion | 32 |
| 4 | Non-contact Tactile Sensing with Optical Mouse Sensor | 34 |
| 4.1 | Introduction | 34 |
| 4.2 | Tactile Sensing | 34 |
| 4.2.1 | Touch Sensor Technology | 37 |
| 4.3 | Primary Idea for Non-contact Tactile Sensing | 47 |
| 4.4 | Experiment Setup | 48 |
| 4.5 | Experiment on Rubber Surfaces | 51 |
| 4.5.1 | Tests on the Two Rubber Surfaces | 51 |
| 4.5.2 | Translation Direction Measurement | 53 |
| 4.5.3 | The Surface Shape of the Object Surface | 56 |
| 4.6 | Experiments on Whitepaper | 57 |
| 4.6.1 | Experiments Procedures | 57 |
| 4.6.2 | Translation Direction Measurement | 58 |
| 4.6.3 | Height Measurement | 59 |
| 4.6.4 | Crack Detection | 60 |
| 4.6.5 | Category Discrimination | 63 |
| 4.7 | Discussion | 64 |
| 4.8 | Conclusion | 66 |

| | | |
|----------|---|-----------|
| 5 | Combined Tactile Sensing with Optical Mouse Sensor | 68 |
| 5.1 | Introduction | 68 |
| 5.2 | Combined Sensing | 68 |
| 5.3 | Experiment | 69 |
| 5.3.1 | Experiment Setup | 69 |
| 5.3.2 | Initial Calibration | 71 |
| 5.3.3 | Experiment Procedures | 73 |
| 5.4 | Analysis | 74 |
| 5.4.1 | Surface Translation Direction Measurement | 74 |
| 5.4.2 | Surface Category Discrimination | 74 |
| 5.4.3 | Surface Height Measurement | 76 |
| 5.4.4 | Summary | 77 |
| 5.5 | Discussion | 78 |
| 5.6 | Conclusion | 80 |
| 6 | Conclusions and Recommendations | 81 |
| 6.1 | Introduction | 81 |
| 6.2 | Recommendations for Future Work | 82 |

List of Figures

| | | |
|-----|--|----|
| 1.1 | Optical mice illuminate an area of the work surface with an LED, to reveal a microscopic pattern of highlights and shadows. These patterns are reflected onto the navigation sensor, which takes pictures at a rate of 1500 images per second or more. | 6 |
| 1.2 | Optical mice illuminate an area of the work surface with an LED, to reveal a microscopic pattern of highlights and shadows. These patterns are reflected onto the navigation sensor, which takes pictures at a rate of 1500 images per second or more. | 7 |
| 2.1 | A robot arm is used to control movement of the optical mouse sensor. | 20 |
| 2.2 | Flowchart of MATLAB application. After the robot arm is started, a short delay is necessary to make the robot arm achieve the status of uniform motion. | 22 |
| 3.1 | Structure of surface shape analyzing device using optical mouse sensor | 26 |

| | | |
|-----|--|----|
| 3.2 | Exploded view drawing of optical mouse components | 27 |
| 3.3 | Experiment system for surface shape analyzing device using optical mouse sensor | 29 |
| 3.4 | Experimental setup (a) and results (b) for smooth slope glass surface | 30 |
| 3.5 | Experimental setup (a) and results (b) for smooth semi cylin- drical acrylic surface. The device is at a height of 20mm to make the height variance of the object surface is in the maxi- mum applicable surface height variance measurement range. . . | 31 |
| 3.6 | Experimental setup (a) and results (b) for sandpaper set MH913. Intuitively, the less the grit size number, the more dispersive the recorded data. | 32 |
| 4.1 | Distance from lens reference plane to surface | 47 |
| 4.2 | Diagram of the experiment system for non-contact tactile sensing | 49 |
| 4.3 | Sensing coordinate systems for non-contact tactile sensing . . | 50 |
| 4.4 | System configuration of mouse in the experiments | 51 |
| 4.5 | 3-D view of the two rubber surfaces used for non-contact tac- tile sensing | 52 |
| 4.6 | Characteristics of resolution vs. height for the rubber surface . | 53 |
| 4.7 | Track curves of different directions for periodically-square- shaped surface | 54 |
| 4.8 | Track curves of different directions for periodically-arc-shaped surface | 54 |
| 4.9 | Different translation directions in non-contact tactile sensing . | 55 |

| | | |
|------|---|----|
| 4.10 | Different texture directions in non-contact tactile sensing . . . | 55 |
| 4.11 | a -axis and b -axis of different resolutions ($\alpha = 70^\circ$) | 56 |
| 4.12 | The relation between the estimated angle α' and the actual angle α | 59 |
| 4.13 | The characteristics of resolution vs. height of whitepaper RHQ-100. | 60 |
| 4.14 | An object surface with specific crack configuration. | 61 |
| 4.15 | The position of the pointer on the display varies with the position of the optical mouse sensor in the y -axis direction. . . . | 62 |
| 4.16 | A forward difference operation is performed on the curve in Fig. 4.15. | 62 |
| 4.17 | Burl Formica, white paper, manila, black copy and black walnut are standard surfaces which Agilent Technologies recommends to be used for surface navigation testing. | 64 |
| 5.1 | Diagram of experiment system for combined tactile sensing . . | 70 |
| 5.2 | Sensing coordinate systems for the combined tactile sensing . . | 72 |
| 5.3 | Height from lens reference plane to surface | 73 |
| 5.4 | Estimated angle vs. actual angle for the surface translation direction measurement | 75 |
| 5.5 | Resolution vs. height characteristics for surface category discrimination | 76 |
| 5.6 | Surface height measurement in the combined tactile sensing . | 77 |
| 5.7 | Diagram of step-by-step sensing procedures in combined tactile sensing | 78 |

List of Tables

| | | |
|-----|---|----|
| 3.1 | Standard deviations of experimental results for sandpaper set | |
| | MH913 | 33 |

Acknowledgements

The author wishes to express his heartfelt gratitude to his supervisor, Professor Katsunori Shida for his valuable guidance, suggestions and encouragement throughout all phases of the research work. It is honorable for the author to be led in the field of sensing technology. It will certainly continue to spur the author on to approach many follow-up researches. Professor Katsunori Shida is an intellectual magnate. The author will always be in awe of his creativity, analysis and comprehension. For last three years he has been a great source of ideas knowledge and feedback for the author. The author also wishes to convey his sincere thanks and deep appreciation to Professor Masatoshi Nakamura, Professor Satoru Goto and Associate Professor Akira Kimoto for their cooperative comments, valuable suggestions and helpful supports while serving as the members of this dissertation committee.

The author would like to thank Associate Professor A. Kimoto and Mr. W. Yoshida for their warm helps to author in the last three years. This thesis is impossible to be completed without their sincerely helps. The author also would like to thank Dr. Chuantong Wang, , Dr. Wei Quan, Dr. Peng Xu for their helps and encouragement. Thanks are also expressed to all the other members of Shida Laboratory for their kindness, helps and encouragement.

The author would like to thank the Japanese Government and Saga University for providing him a very valuable chance for his study period in Japan. Finally, the author conveys his heartfelt thanks to his parents and relatives for their prayers and blessings helped him to overcome all the difficulties while being away from them.

Abstract

In 1999, Agilent Technologies introduced the first optical position sensor for mouse technology in the world. Besides functioning as part of a pointing device in computing, an optical mouse sensor can be considered as a general optical position sensor. One major drawback with the majority of optical displacement measuring tools lies with their relative high cost. Due to the economics of large volume production, the cost of an optical mouse sensor is extremely low.

The optical mouse sensor has been shown to be able to provide highly accurate measurements of slow displacements with a resolution of 0.0635 mm. Its efficiency for vibratory displacements sensing is also investigated and the work concludes that the optical mouse technology currently available is workable, but has a confined scope of low frequency and low amplitude application in vibration motion sensing. As an optical position sensor, the optical mouse sensor has found positions in many industry applications. The optical mouse sensors are experimentally characterized in view of their use as multiple degree of freedom sensors for industrial application. In mobile robot applications, the optical mouse sensors have been employed for odometry measurement. In medical field, three optical mouse sensors are used to measure the movements of a device for tracking minimally invasive surgical (MIS) instruments in training setup. In neuroscience research, it is employed by an inexpensive submillisecond system for walking measurements of small animals. In microscopy field, it has been used as a region-of-interest position

recorder and used in a digital readout manometer. In chemical field, it has been employed to measure viscoelastic deformation.

In this thesis, the optical mouse sensor is used for surface shape analyzing, non-contact tactile sensing and combined tactile sensing respectively.

Firstly, the optical mouse sensor is employed for surface shape analyzing. Besides of the flexible use of the optical mouse sensor, the proposed device is characterized by a small sensing area derived from the use of a ballpoint pen. The minimum of detectable height variance is restricted by the size of the ballpoint and the resolution of the optical mouse sensor. Experiments show that the proposed device can record the shape of smooth surface digitally and evaluate the roughness of rough surface statistically.

Secondly, the optical mouse sensor is employed for non-contact tactile sensing. It is an interesting idea to make an optical mouse sensor work in the manner of a human hand but in a non-contact way to "feel" the object surface. For the experiments on rubber surfaces, a periodically-square-shaped rubber surface and a periodically-arc-shaped rubber surface are studied in the experiments. Experiments show that the shape information of the object surfaces and the translation direction of the object surfaces can be obtained at the same time. For experiments on whitepaper, the translation direction, the height and the category of an object surface can be sensed. Based on the data table obtained from the experiments, the translation direction is calculated and the nonlinearity of the translation direction sensing is studied. It can be concluded that the resolution of an optical mouse sensor is direction-related. The feasibility of surface height measurement is analyzed and the optical mouse sensor can be used for crack detection on a plane surface. Height

variation of 0.2mm can be detected. Besides, the feasibility of the optical mouse sensor for surface discrimination is proposed.

Thirdly, the optical mouse sensor is employed for combined tactile sensing . Based on the experimental characteristics of the optical mouse sensor, with a step-by-step table-look-up method, a combined tactile sensing system is proposed. When an object surface is moved underneath the optical mouse sensor, the translation direction, the category and the height of the object surface can be obtained with the recorded output of the optical mouse sensor based on a predefined data table.

There are following advantages for the optical mouse sensor. The sensor interface is ready for use. The output of the system is digital, without the need of any additional analog-to-digital component. The driver and software for the sensing system is easily available. The outputs of the sensor can be intuitively displayed on the display and recorded on the hard disk, which greatly improves the convenience of the system. Because of the large-scale manufacture of the optical mouse sensor, the sensing system is cost-effective, and thus is easily available and generalized.

Chapter 1

Introduction

1.1 Optical Mouse

In computing, a mouse is a pointing device that functions by detecting two-dimensional motion relative to its supporting surface. Physically, a mouse consists of a small case, held under one of the user's hands, with one or more buttons. It sometimes features other elements, such as "wheels", which allow the user to perform various system-dependent operations, or extra buttons or features can add more control or dimensional input. The mouse's motion typically translates into the motion of a pointer on a display, which allows for fine control of a Graphical User Interface.

The name *mouse*, originated at the Stanford Research Institute, derives from the resemblance of early models (which had a cord attached to the rear part of the device, suggesting the idea of a tail) to the common mouse.

Today's computer mouse comes in many shapes, and in a wide range of features, sizes and prices. The two main technologies driving this input

device are optical and mechanical. The mechanical engine was the earlier system and was introduced in the 1960s. Optical technology was introduced in the 1980s but didn't gain much traction until the early part of 2000.

Since then, with the massive adoption of computers for communication, data storage, and networking, the mouse's function as an input device has grown increasingly more critical particularly in accommodating the higher tracking speeds and better response required by demanding users.

Fueled by this insatiable appetite for performance, the mouse has come a long way from its humble beginnings. From a single button, corded device, now there is a version for every type of user including cordless models, and even high performance models oriented toward gaming.

1.1.1 The Birth of the Computer Mouse

The mouse was invented by Douglas Engelbart and developed the first one with his Chief Engineer, Bill English, of Stanford Research Institute (now SRI international) in 1963. It was intended as an input device for Engelbart's oNLine System (NLS). Their creation used two perpendicular wheels attached to potentiometers to track its movement along the horizontal and vertical axes.

In 1971, Xerox Palo Alto Research Center (PARC) signed an agreement with SRI licensing Xerox to use the mouse. The Xerox PARC mouse replaced the external wheels with a single ball, which could rotate in any direction. The ball's motion was detected using perpendicular wheels connected to electrical commutators to move the onscreen cursor. The first Alto mouse was

operational in 1972. Today's mechanical mouse owes a great deal to this Xerox PARC design.

A couple of reasons for the slow adoption of mice from the 1970s to the early 1980s were the limited number of personal computers in the market, as well as their high prices. The Xerox PARC mouse in those days would set a buyer back a whopping \$400 and required an additional \$300 computer interface.

Another milestone in mechanical mouse history came through Apple. Unlike prior mouse designs that used electrical commutators, the Apple mouse used optical encoders along the ball's equator, 90 degrees apart.

Microsoft made its debut in the mouse market in 1983. Known as the "Green Eye Mouse", the main function of this mouse was to provide navigation support for the GUI context of Microsoft Word for MS-DOS v. 1.00. The mouse has two protruding green buttons, hence its "green eye" nickname, and was equipped with a 25-pin D-plug to attach to the serial port on the original PC and compatibles. On the underside it had three small steel balls that allowed it to glide over a surface and a large steel ball in the center to register its position.

One of the earliest optical mouse design started with the Mouse Systems model. Commercially available from 1982 to 1995, this mouse used a four-segment photodiode chip, and could only be used on a special mirrored surface having a grid of fine lines. Ultimately several versions were available for Amiga computers, while other versions were packaged with a PS/2 connector to hook-up with an IBM PC or compatible.

Then in 1985, Xerox introduced the 6085 Star, which featured the first

optical mouse that was not tied to a precision surface. Although it was supplied with a pad having a printed dot pattern, it would also operate on other surfaces that had high-contrast printing. It could not, however, work on ordinary random surfaces such as most mouse pads or tabletops.

In 1999, Agilent Technologies introduced a revolutionary optical position sensor. This innovative sensor operates by actually "taking a picture" of the surface on which it is navigating, and comparing images sequentially to detect the speed and direction of movement. The device is able to navigate on a wide variety of surfaces, freeing the user from the space limitation of any mouse pad.

Enhancing the optical technology, in September 2004, Agilent (now Avago Technologies) revealed laser illumination and tracking technology. Providing more surface tracking power than LED-based optical mice, laserbased optical mice with Avago LaserStream technology can easily track on painted metal, translucent plastics, frosted glass and many other previously difficult to navigate surfaces. Avago's laser engines also have increased navigation performance compared to position sensors using LED illumination. Boasting some of the highest performance benchmarks, including motion velocity up to 45 inches per second, frame rates in excess of 7,000 frames per second and a high resolution of 2,000 counts-per-inch, mouse performance has been bumped up a couple of notches.

1.2 Optical Mouse Sensor

The mechanical computer mouse, Douglas Engelbart's invention of the 1960's, is starting to look like an endangered species. While users praise its ingenuity, many resent its unreliability and its need for frequent cleaning.

Change is on the way. Thanks to advances in optical navigation, solid-state optical mice have become the new standard. These new mice never need cleaning, track precisely and work on nearly all surfaces. They may even reduce repetitive stress injury, and to most people they just plain feel better.

Their ease of use belies their complexity. Hidden inside the sleek plastic case is a sophisticated design, combining the best of today's electronic and optical technology.

1.2.1 Inside An Optical Mouse

If you took apart an optical mouse and looked inside, you'd find a complete imaging system. The mouse is essentially a tiny, high-speed video camera and image processor.

As shown in Fig.1.1, a light-emitting diode (LED) illuminates the surface underneath the mouse. The light from the LED reflects off microscopic textural features in the area.

A plastic lens collects the reflected light and forms an image on a sensor. If you were to look at the image, it would be a black-and-white picture of a tiny section of the surface. The sensor continuously takes pictures as the mouse moves. The sensor takes pictures quickly 1500 pictures (frames) per

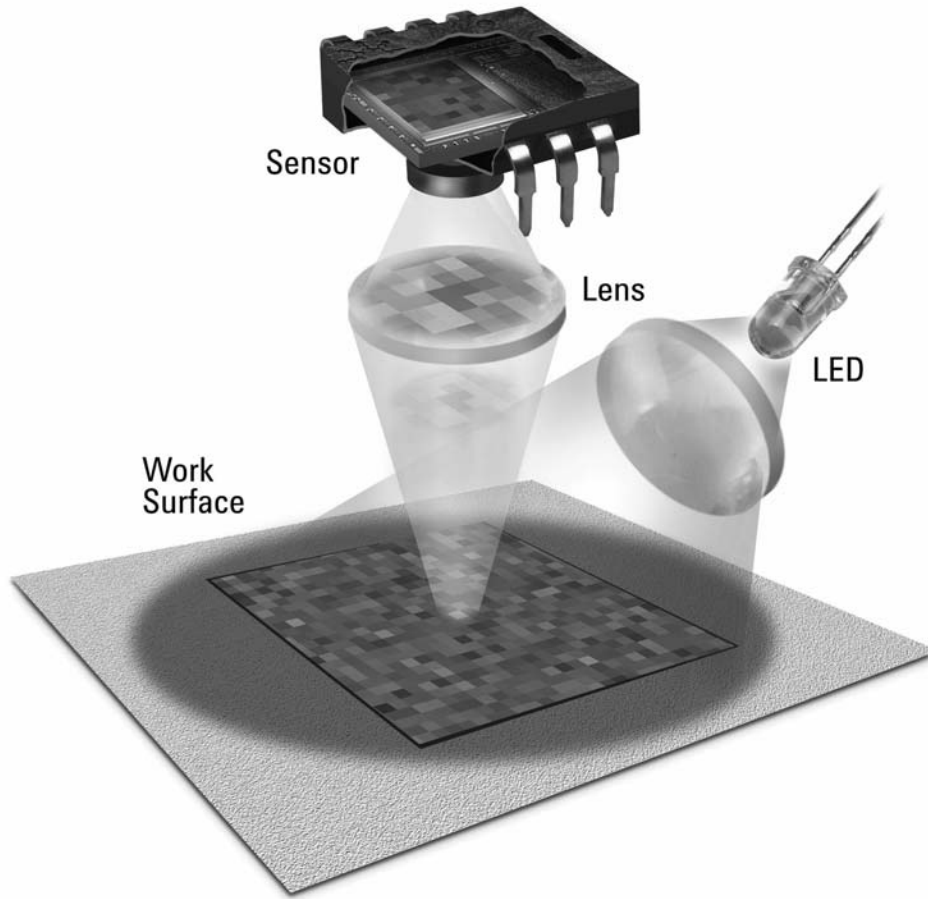


Figure 1.1: Optical mice illuminate an area of the work surface with an LED, to reveal a microscopic pattern of highlights and shadows. These patterns are reflected onto the navigation sensor, which takes pictures at a rate of 1500 images per second or more.

second or more fast enough so that sequential pictures overlap. The images are then sent to the optical navigation engine for processing.

1.2.2 The Basics of Optical Navigation

The optical navigation engine is the brain of an optical mouse sensor. It identifies texture and other features in the pictures and tracks their motion. Much of the same visual material can be recognized in both frames. The underlying technology is to determine optical flow.

Fig.1.2 illustrates how this is done. Two images were captured sequentially as the mouse was panned to the right and upwards. Much of the same visual material can be recognized in both frames. Through a patented image-processing algorithm, the optical navigation engine identifies common features between these two frames and determines the distance between them. This information is then translated into X and Y coordinates to indicate mouse movement.

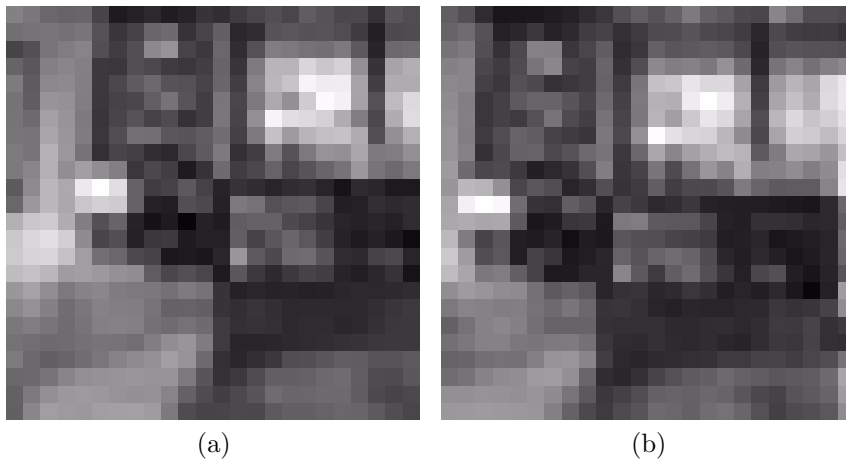


Figure 1.2: Optical mice illuminate an area of the work surface with an LED, to reveal a microscopic pattern of highlights and shadows. These patterns are reflected onto the navigation sensor, which takes pictures at a rate of 1500 images per second or more.

1.2.3 Advantages of Optical Technology

Unlike traditional mechanical mice, optical mice have no moving ball that can clog up with dust or dirt. Users no longer need to perform regular cleaning for accurate tracking. In addition, optical technology can work on many surfaces where ball mice have difficulty, including curved surfaces or soft fabric. Because of their distinct advantages, optical mice are fast becoming the standard in computer stores around the world.

1.3 Optical Position Sensor

A wide variety of displacement sensors have been developed based on the principles of capacitive, inductive, magnetic, ultrasonic and optical sensing. For displacement sensors based on the optical effect alone, designs have been reported employing the principles of triangulation [7, 19], interferometry [39, 41], moire [2, 21], diffraction [8, 35], time-of-flight [23], and speckle [27, 42]. Some of these schemes are able to provide measurements with sub-micrometer accuracy. Nevertheless, not all applications require such high degrees of measurement accuracy. In building drift monitoring and large-strain viscoelastic measurements, for example, mensurations in the range of 0.1 mm are generally sufficient. One major drawback with the majority of optical displacement measuring tools lies with their relative high cost. This arises primarily from the expensive components used in certain designs and the non-economics of scale associated with low volume manufacturing of such systems. There is, hence, an incentive to source for alternative cost-effective optical sensors for displacement measurement; in particular,

when the demands of accuracy are not very high.

The optical mouse sensor is used to implement a non-mechanical tracking engine for computer mice. It is based on optical navigation technology, which measures changes in position by optically acquiring sequential surface images (frames) and mathematically determining the direction and magnitude of movement.

1.4 Application of Optical Mouse Sensor

Computer mouse device manufacturing plays an important role in computer peripheral industry. In 1999, Agilent Technologies introduced the first optical position sensor for mouse technology in the world.

Besides functioning as part of a pointing device in computing, an optical mouse sensor can be considered as a general optical position sensor. One major drawback with the majority of optical displacement measuring tools lies with their relative high cost. Due to the economics of large volume production, the cost of an optical mouse sensor is extremely low.

The use of the computer mouse for scientific work has been previously reported [10,33,34]. The majority of these involve studies on visual tracking and human motor control [1,6].

Optical sensors are used extensively for displacement measurement. A cost-effective optical displacement sensor will be invaluable in applications where very high resolutions are not required. The optical mouse has been investigated to determine its suitability for two-dimensional displacement measurement [28]. While the mouse worked only on objects with opaque

surfaces, experiments conducted with a commercial unit with 0.0635 mm resolution showed that highly linear (average R^2 -value of 0.9914) and low error (mean square error (M.S.E.) value below 0.018 mm²) measurements could be attained [26]. On the flipside, the unit could only operate if placed at a distance no greater than 1.25 mm from the object surface. Overall, the optical mouse has been found to be a viable two-dimensional displacement sensor. Its efficacy was demonstrated in measuring the viscoelastic elongation of polyethylene. While the viscoelastic behavior of materials is well studied, it is still actively researched due to its importance in a wide spectrum of engineering applications [12, 18]. Optical methods to determine the viscoelastic deformation of materials have often relied on expensive and complicated designs.

The optical mouse has been previously shown to be able to provide highly accurate measurements of slow displacements with a commercial unit with 0.0635 mm resolution. Its efficiency for vibratory displacements is also investigated [30]. It was found that frequency and amplitude thresholds existed beyond which the position-time distributions obtained would not permit analysis. From the analyzable distributions derived, frequency estimation errors below 15% in magnitude could only be comfortably achieved if the frequency was limited to 35 Hz and the amplitude limited to 0.4 mm, while amplitude estimation errors below 20% in magnitude could only be safely attained if the frequency was limited to 5 Hz and the amplitude limited to 0.2 mm. It concludes that the optical mouse technology currently available is workable, but has a confined scope of low frequency and low amplitude application in vibration motion sensing. Nevertheless, this range still makes

it useful as a dynamic sensor in a reasonable number of applications where low cost is particularly required.

The optical mouse is an extremely cost-effective displacement sensor. In [31] the author describes the use of an optical mouse in an experiment to record position as a function of time for a simple mechanical oscillator. The recorded data correspond closely to that expected for damped harmonic oscillations. These measurements can be made without the use of cumbersome attachments. The optical mouse is also advantageous in obviating concern about the integrity of electrical contact points and the deleterious effects of wear and of dirt accumulation on moving parts.

A simple demonstration of viscoelasticity can be carried out by attaching a weight to a polymer film and watching it extend over time. For accurate and quantifiable data on the deformation, an electronic displacement sensor should be incorporated. Most of such sensors are expensive. In [29], an optical mouse was demonstrated to provide accurate data at low cost.

The original mouse only had two wheels attached to encoders to measure horizontal and vertical displacement whereas the simplest and effective way to measure the displacement and trajectory of a mobile robot is to use an encoder placed in the drive motors, [3, 17, 24] in the active wheels or even in additional passive wheels. However, encoder measurements suffer from problems of accurate wheel diameter estimation, uncertainty in the determination of the contact point with the floor, dirt accumulation and wheel wear and slippage.

In mobile robot applications, these problems play an important role because the goal is to measure the robot displacement with the maximum ac-

curacy. To solve these problems additional sensors, such as ultrasonic, laser measurement system and vision [5] and are widely used to extract and compare additional relative scenario information to correct the estimated robot position.

The optical mouse is proposed for indoor odometry measurement in mobile robot applications [9, 13, 15, 16, 36, 37]. The optical mouse is a very low-cost sensor and has the advantage that the measured displacement is independent from the kinematics of the robot because the optical sensor uses external natural microscopic ground landmarks to obtain the effective relative displacement. The sensor is calibrated and evaluated for odometry measurement. It was found that the original conception inside a visual feedback loop precludes its use as an isolated displacement sensor although its impressive speed and parts, with a CMOS camera and a digital signal processor embedded on the same chip, suggests that an improved design can be a good alternative for accurate mobile robot odometry measurement.

A novel, four degrees of freedom, low-cost device for tracking minimally invasive surgical instruments (MIS) in training setups was developed [22]. This device consists of a gimbal mechanism with three optical computer mouse sensors. The gimbal guides the MIS instrument, while optical sensors measure the movements of the instrument. To test the feasibility of using optical mouse sensors to track MIS instruments, the accuracy of these sensors was tested depending on three conditions: distance between lens and object, velocity of movements, and surface characteristics. The results of this study were used for developing a prototype TrEndo. Tests performed on TrEndo show that the smallest movement that can be recognized by sensors is 0.06

mm for translation and 1.27° for rotation of the MIS instrument around its axis. The smallest recognized angle for rotation around incision point is 0.23° . The accuracy of TrEndo is higher than 95%, and therefore allows tracking the movements of the MIS instrument.

Low-cost optical motion sensors commonly used in computer mice are experimentally characterized in view of their use as multiple degree of freedom sensors for industrial applications [25]. Each non-contact optical sensor provides two output channels giving x and y components of the device relative displacement. The experimental activity presented in the paper shows that limitations mainly arise from the device sensitivity to the reference surface texture and from the upper limited working speed. It is shown that, for an effective application, the surface over which the sensor is moving must be cooperative. In case of a typical commercial device working on a white surface, the linearity error evaluated over a single pass trajectory of 200 mm is about 0.1% whilst the variability due to the reference surface pattern orientation is of 2%.

The need for simultaneous measurement of multiple degree-of-freedom (DOF) motions can be found in numerous applications such as robotic assembly, precision machining, optical tracking, wrist actuators, and active joysticks. Conventional single-axis encoders, though capable of providing high-resolution (linear or angular) measurements, rely on mechanical linkages (that often introduce frictions, backlashes, and singularities) to constrain the device so that the three-DOF (3-DOF) motion can be deduced from the individual orthogonal measurements. The authors present here a noncontact optical sensor for 3-DOF planar and spherical orientation measurements [20].

The authors begin with the operational principle of a microscopic-surface-based optical sensor, that is optical mouse sensor. The design concept and theory of a dual-sensor system capable of measuring 3-DOF planar and spherical motions in real time are then presented. Along with a detailed analysis, the concept feasibility of two prototype 3-DOF dual-sensor systems for measuring the instantaneous center of rotation and the angular displacement of a moving surface is demonstrated experimentally. It is expected that the analysis will serve as a basis for optimizing key design parameters that could significantly influence the sensor performance.

Stimuli from a broad spectrum of sensory modalities, including visual, auditory, thermal, and chemical, can elicit walking responses in animals, reflecting neural activity in sensorimotor pathways. The authors have developed an integrated walking measurement system with sub-millisecond temporal accuracy capable of detecting position changes on the order of 0.1 mm [11]. This tracking system provides the experimenter with a means by which to map out the response spectrum of a tethered animal to any number of sensory inputs on time scales relevant to propagation in the nervous system. The data acquisition system consists of a modified optical computer mouse, a microcontroller with peripheral support circuitry, a binary stimulus sync line, and a serial (RS-232) data transfer interface. The entire system is constructed of relatively inexpensive components mostly converted from commercially available peripheral devices. The authors have acquired walking data synchronized with auditory stimuli at rates in excess of 2100 samples per second while applying this system to the walking phonotactic response of the parasitic fly *Ormia ochracea*.

In optical microscopy, the microscopic features of interest typically have to be derived from regions that are spatially distributed over the sample. While the features to be analyzed may be minute, the regions from where they must be obtained from may be located quite far apart from one another. If the features are not distinct enough to allow easy visual discrimination, it would be tedious and time-consuming to attempt to recall and revisit these regions of interest. One method to overcome this difficulty would be to note and record the graduated markings on the microscope, or to use built-in position encoders. The former is tedious while the latter is generally expensive. A region-of-interest position-recording implement based on the use of an optical mouse is presented [32]. It is inexpensive and easily adaptable to the manual stage of any optical microscope.

The manometer remains a useful pressure measuring instrument in the laboratory and in industry despite it being discovered centuries ago. One of the major limitations of this instrument lies with its inability to produce digital readouts for automated data acquisition. The authors demonstrate this ability via the incorporation of an optical mouse to sense liquid level movement. The approach is very easy to implement and inexpensive. It is also shown to be able to provide digital pressure measurements with good accuracy and repeatability [38].

In [4], the authors presents a novel sensor for classification of material type and its surface roughness. The sensor is developed by means of a lightweight plunger probe and an optical mouse. An experimental prototype was developed which involves bouncing or hopping of the plunger based impact probe freely on the plain surface of an object under test. The time and

features of bouncing signal are related to the material type and its surface properties, and each material has a unique set of such properties. During the bouncing of the probe, a time varying signal is generated from optical mouse that is recorded in a data file on PC. Some dominant unique features are then extracted using digital signal processing tools to optimize neural network based classifier used with the sensor. The classifier is developed on the basis of application of supervised structures of neural networks. For this, an optimum multilayer perceptron neural network (MLP NN) model is designed to maximize accuracy under the constraints of minimum network dimension. The optimal parameters of MLP NN model based on various performance measures and classification accuracy on the testing datasets even after attempting different data partitions are determined. The classification accuracy of MLP NN is found reasonable consistently in respect of rigorous testing using different data partitions. The performance of the proposed MLP NN based classifier has also been compared with the statistical classification trees approach. It is seen that the former one clearly outperforms the statistical approach.

1.5 Our Work

Our work can be divided into 3 parts.

In Chapter 3, the optical mouse sensor is employed for surface shape analyzing. Besides of the flexible use of the optical mouse sensor, the proposed device is characterized by a small sensing area derived from the use of a ballpoint pen. The minimum of detectable height variance is restricted

by the size of the ballpoint and the resolution of the optical mouse sensor. Experiments show that the proposed device can record the shape of smooth surface digitally and evaluate the roughness of rough surface statistically.

In Chapter 4, the optical mouse sensor is employed for non-contact tactile sensing. It is an interesting idea to make an optical mouse sensor work in the manner of a human hand but in a non-contact way to "feel" the object surface. For the experiments on rubber surfaces, a periodically-square-shaped rubber surface and a periodically-arc-shaped rubber surface are studied in the experiments. Experiments show that the shape information of the object surfaces and the translation direction of the object surfaces can be obtained at the same time. For experiments on whitepaper, the translation direction, the height and the category of an object surface can be sensed. Based on the data table obtained from the experiments, the translation direction is calculated and the nonlinearity of the translation direction sensing is studied. It can be concluded that the resolution of an optical mouse sensor is direction-related. The feasibility of surface height measurement is analyzed and the optical mouse sensor can be used for crack detection on a plane surface. Height variation of 0.2 mm can be detected. Besides, the feasibility of the optical mouse sensor for surface discrimination is proposed.

In Chapter 5, the optical mouse sensor is employed for combined tactile sensing . Based on the experimental characteristics of the optical mouse sensor, with a step-by-step table-look-up method, a combined tactile sensing system is proposed. When an object surface is moved underneath the optical mouse sensor, the translation direction, the category and the height of the object surface can be obtained with the recorded output of the optical mouse

sensor based on a predefined data table.

Chapter 2

Technical Introduction

This chapter introduces the hardware and software tool employed in the development of the thesis. These tools lay a solid foundation for the whole research work.

2.1 Robot Arm

In our study, to make the sensor move in a uniform speed, a robot arm is used to control movement of the optical mouse sensor, as shown in Fig. 2.1.

A robot arm of model VS-6354DM is controlled by a robot controller of model RC5-VS6A. In each of X, Y and Z directions, the position repeatability of the robot arm of model VS-6354DM is $\pm 0.02\text{mm}$.

2.2 MATLAB and Pointer Tracking

One of basic task of our study is to programm to track the mouse pointer on the screen.



Figure 2.1: A robot arm is used to control movement of the optical mouse sensor.

MATLAB is a high-level language and interactive environment that enables you to perform computationally intensive tasks faster than with traditional programming languages such as C, C++, and Fortran.

In graphics, MATLAB supports Handle Graphics. Graphics objects are the basic elements used to display graphics and user interface elements. One of the graphics objects is *root*, that is top of the hierarchy corresponding to the computer screen.

The main property of the root we used in the program to track the pointer is *PointerLocation*.

[**x,y**]

Current location of pointer. A vector containing the x- and y-coordinates of the pointer position, measured from the lower left corner of the screen. You can move the pointer by changing the values of this property. The Units property determines the units of this measurement.

This property always contains the current pointer location, even if the pointer is not in a MATLAB window. A callback routine querying the *PointerLocation* can get a value different from the location of the pointer when the callback was triggered. This difference results from delays in callback execution caused by competition for system resources.

The flowchart of the MATLAB application for data recording is shown in Fig. 2.2. After the robot arm is started, a short delay is necessary to make the robot arm achieve the status of uniform motion.

An instance of the experiments is as follows:

1. Start the MATLAB application;
2. Start the robot arm VS-6354DM;
3. After a short acceleration, the optical mouse sensor reached the uniform motion stage, and the recording is started by the MATLAB application automatically;
4. The obtained data are stored in the hard disk for further analysis.

The output of the sensing system is a sequence (x_i, y_i) , which describes the track of the pointer on the computer screen. Index i is integers in the interval $[1, 1000]$, x is in the interval $[1, 1024]$ and y is in the interval $[1, 768]$.

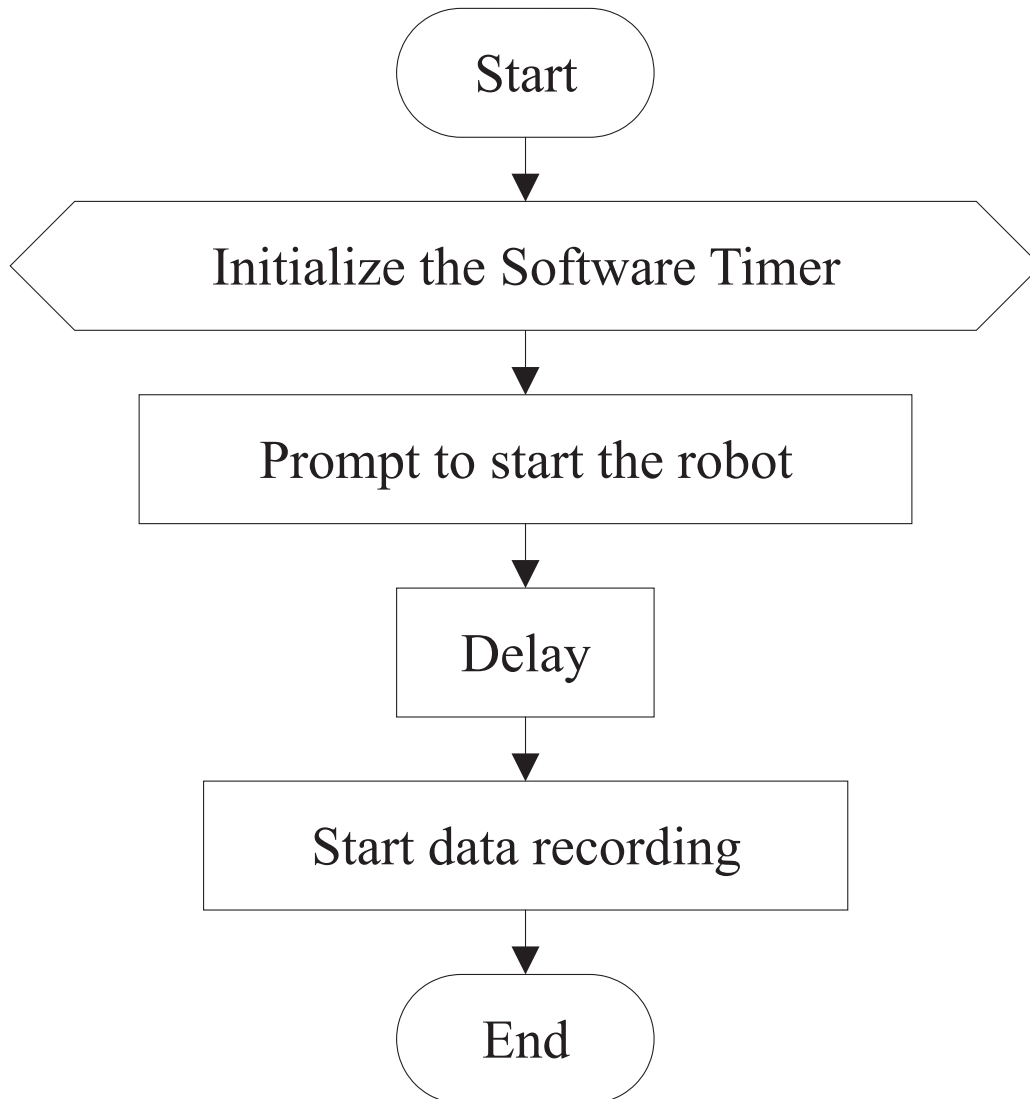


Figure 2.2: Flowchart of MATLAB application. After the robot arm is started, a short delay is necessary to make the robot arm achieve the status of uniform motion.

Chapter 3

Surface Shape Analyzing

Device Using Optical Mouse

Sensor

3.1 Introduction

The main objective of the study is to propose a device to analyze the surface shape with flexible use of an optical mouse sensor.

Instead of functioning as part of a pointing device in computing, an optical mouse sensor is used in the proposed device for surface shape analyzing. Besides of the flexible use of the optical mouse sensor, the proposed device is characterized by a small sensing area derived from the use of a ballpoint pen. The minimum of detectable height variance is restricted by the size of the ballpoint and the resolution of the optical mouse sensor. Experiments show that the proposed device can record the shape of smooth surface digitally

and evaluate the roughness of rough surface statistically.

3.2 Sandpaper

Sandpaper is a form of paper where an abrasive material has been fixed to its surface.

Sandpaper is part of the "Coated abrasives" family of abrasive products. It is used to remove small amounts of material from surfaces, either to make them smoother (painting and wood finishing), to remove a layer of material (e.g. old paint), or sometimes to make the surface rougher (e.g. as a preparation to gluing).

3.2.1 Grit Sizes

Grit size refers to the size of the particles of abrading materials embedded in the sandpaper. A number of different standards have been established for grit size. These standards establish not only the average grit size, but also the allowable variation from the average. The two most common are the United States CAMI (Coated Abrasive Manufacturers Institute, now part of the Unified Abrasives Manufacturers' Association) and the European FEPA (Federation of European Producers of Abrasives) "P" grade. The FEPA system is the same as the ISO 6344 standard. Other systems used in sandpaper include the Japan Industrial Standards Committee (JIS), the micron grade (generally used for very fine grits). The "ought" system was used in the past in the United States. Also, cheaper sandpapers sometimes are sold with nomenclature such as "Coarse", "Medium" and "Fine", but it

is not clear to what standards these names refer.

3.3 Device Structure

The structure of the proposed device is illustrated in Fig.3.1. The heart of the device is an optical mouse sensor ADNS-2051. The ADNS-2051 can determine the direction and magnitude of movement at the maximum of 800 dots per inch (dpi) and at speeds up to 14 inches per second. The ADNS-2051 contains an Image Acquisition System (IAS), a Digital Signal Processor (DSP), a two-channel quadrature output, and a two-wire serial port. The IAS acquires microscopic surface images via the lens and illumination system provided by the HDNS-2100 lens, HDNS-2200 clip, and HLMP-ED80-XXXXX LED. These images are processed by the DSP to determine the direction and distance of motion. The DSP generates the Δx and Δy relative displacement values that are converted into two channel quadrature signals.

The exploded view drawing of the above-mentioned optical mouse components is illustrated in Fig. 3.2. The HDNS-2200 clip provides optical and mechanical coupling of the LED to the HDNS-2100 lens. The clip also provides a mechanical compression feature which locates over the ADNS-2051 sensor and is used to ensure that a light mechanical contact is always maintained between the ADNS-2051 sensor and the HDNS-2100 lens when assembled. The PCB provides the interface circuit between the ADNS-2051 sensor and the computer to transmit the output of the ADNS-2051 sensor to the computer. The base plate is embedded into the housing of the device.

In the housing, there is a slipper block. The slipper block is wooden and

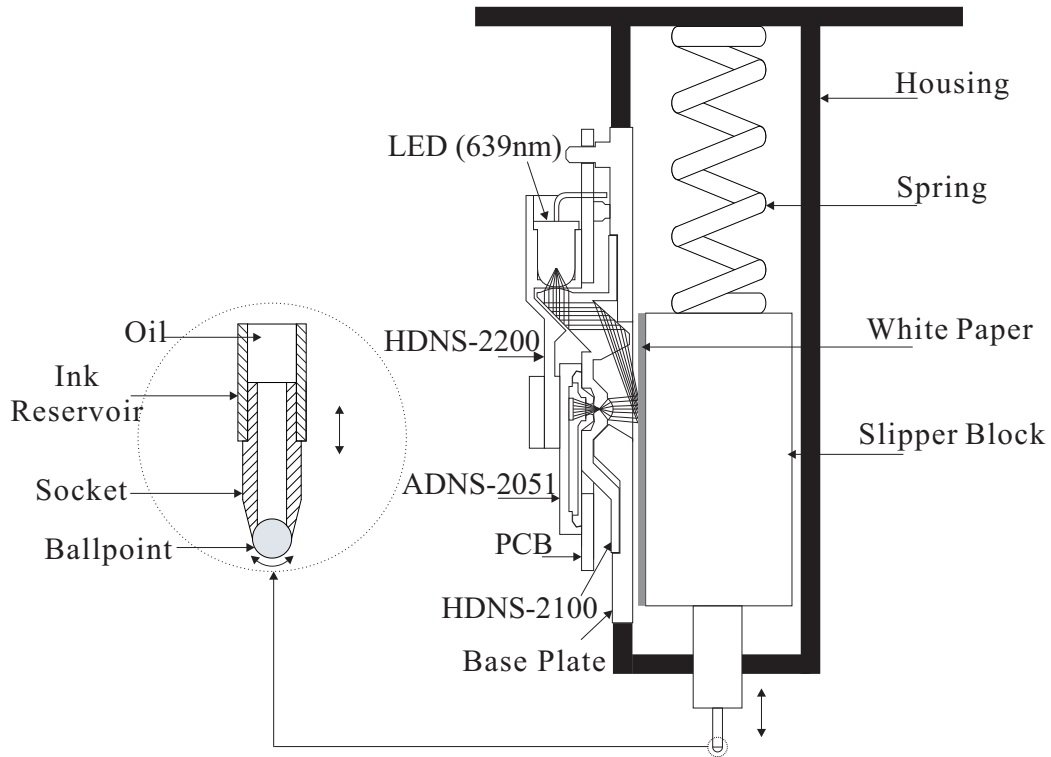


Figure 3.1: Structure of surface shape analyzing device using optical mouse sensor

therefore of less inertia. Compared with the wooden surface, the white paper surface is a more responsive work surface for the optical mouse sensor, and therefore a piece of white paper as the work surface is attached to the wooden surface next to the optical mouse sensor.

Specially, at the bottom of the slipper block, part of a ballpoint pen is used as the "antenna". The structure of the ballpoint pen is just right a nice and low-cost mechanical structure to keep a smooth mechanical contact between the "antenna" and the object surface. Besides, at the top of the slipper block, a spring is attached to keep a durative mechanical contact between the ballpoint and the object surface. When the device sweeps the object

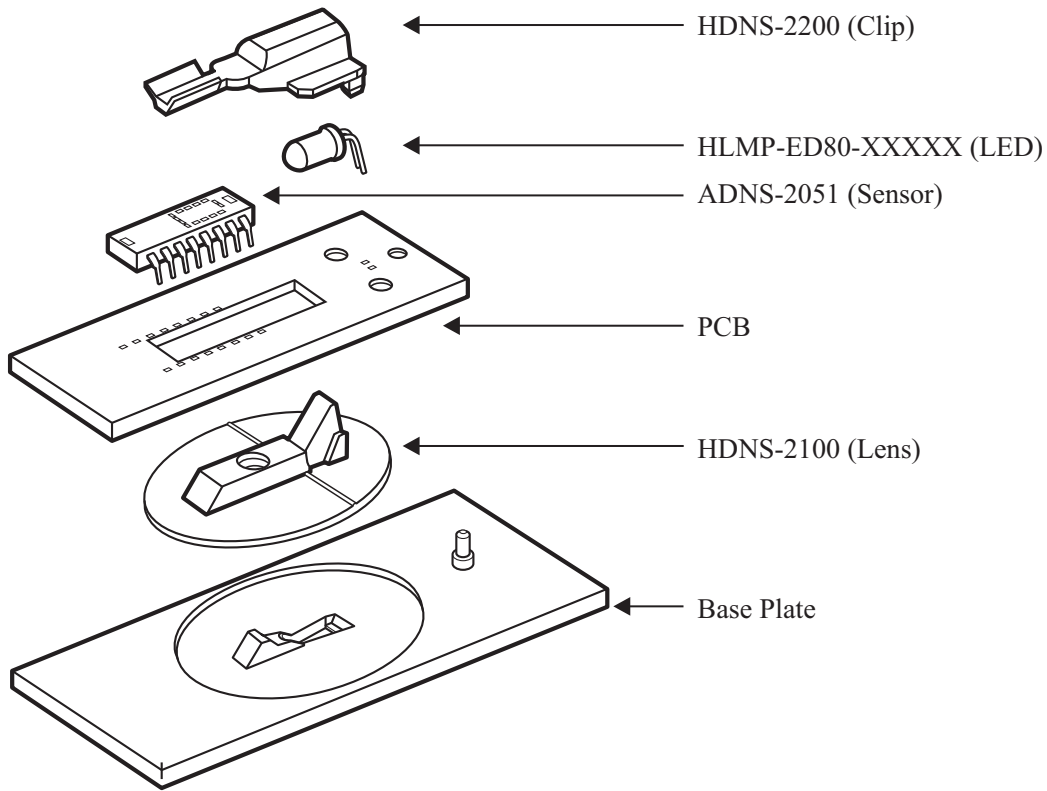


Figure 3.2: Exploded view drawing of optical mouse components

surface, the optical mouse sensor stays fixed while the slipper block moves up and down responding to the height variances of the object surface. The maximum applicable surface height variance measurement range is restricted by the working range of the spring, and here it is about 15mm. The minimum of detectable height variance is restricted by the size of the ballpoint and the resolution of the optical mouse sensor. The smaller the size of the ballpoint and the higher the resolution of the optical mouse sensor, the smaller the minimum of detectable height variance.

3.4 Experiments

The experiment system shown in Fig. 3.3 is set up to test the proposed device. A robot arm of model VS-6354DM is controlled by a robot controller of model RC5-VS6A. In each of X, Y and Z directions, the position repeatability of the robot arm of model VS-6354DM is $\pm 0.02\text{mm}$. The device is held by the robot arm and is connected to a computer through a USB cable. On the computer, a MATLAB program is developed to record the position of the pointer on the screen. The test object surface is fixed on the platform.

A typical experiment instance is as follows: the proposed device held by the robot arm sweeps the object surface horizontally at a speed of 1mm/s , while the MATLAB application records the pointer position on the screen with a sampling interval of 0.1s .

Before comprehensive tests on the device, the relative position between the robot arm and the platform are adjusted until the recorded data responding to a smooth flat glass surface as reference surface are constant in the y axis on the screen during the experiment sampling time-interval.

Three kinds of object surface are prepared to test the proposed device. It is the relative displacement of the pointer on the screen that makes sense. In order to unify the data processing, the first data point of each recorded data sequence is considered as zero displacement.

Firstly, a smooth slope glass surface shown in Fig. 3.4 (a) is selected as a typical flat surface. As shown in Fig. 3.4 (b), the device shows good linearity with $R = 0.9985$.

Some adjacent sampling points keep the same value is because that the

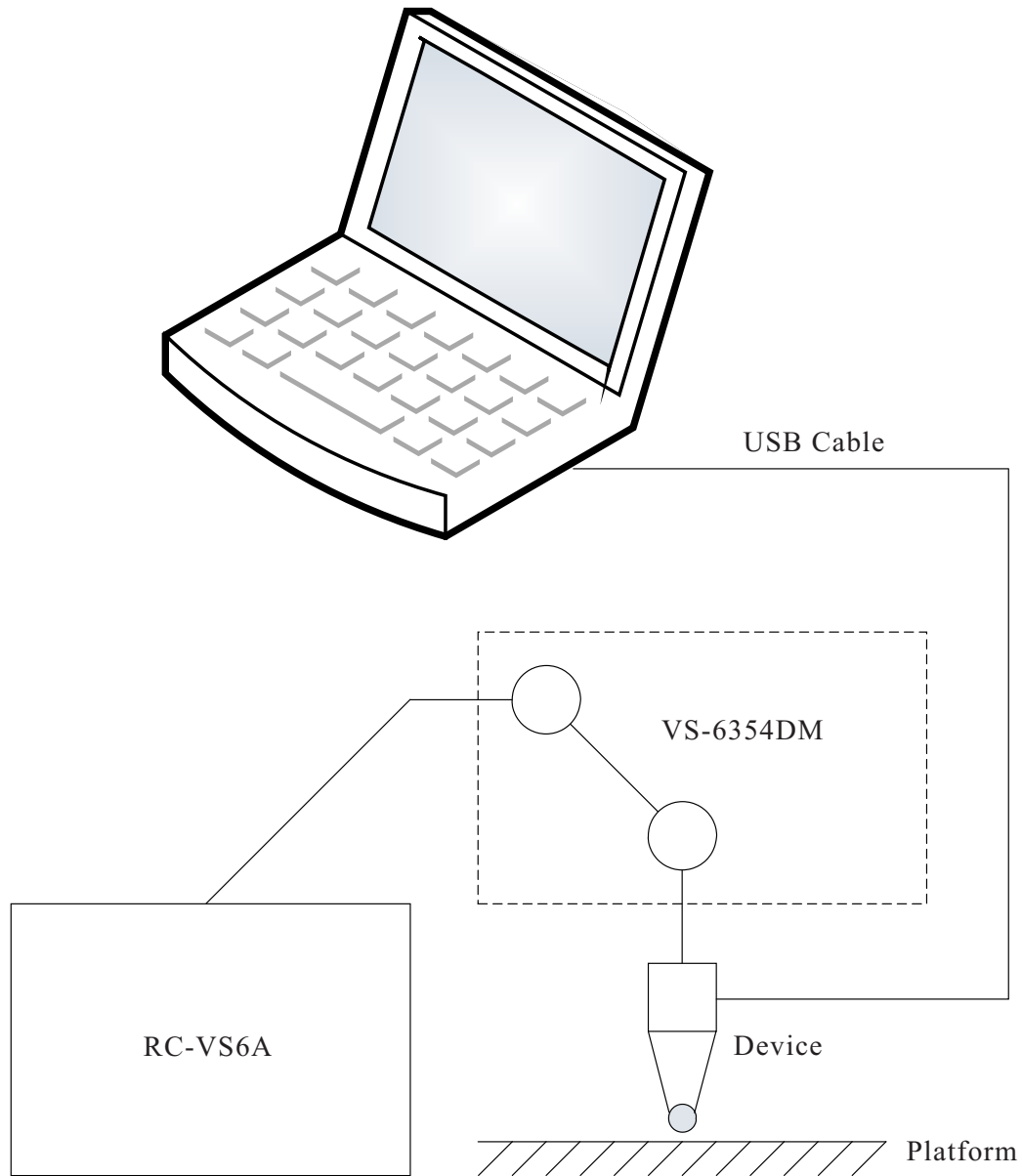


Figure 3.3: Experiment system for surface shape analyzing device using optical mouse sensor

height variance is less than the minimum of detectable height variance.

Secondly, a smooth semi cylindrical acrylic surface shown in Fig. 3.5 (a) is selected as a typical curved surface. The recorded data are shown in Fig.

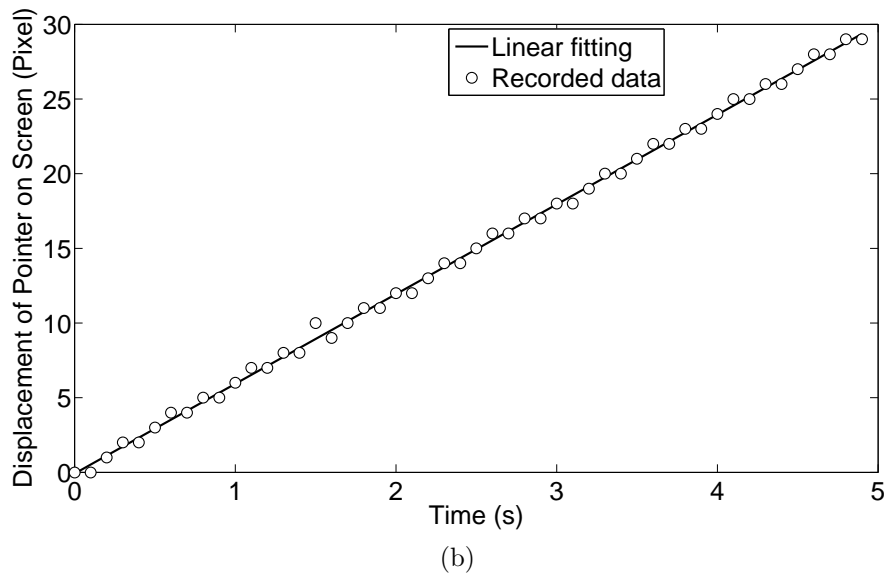
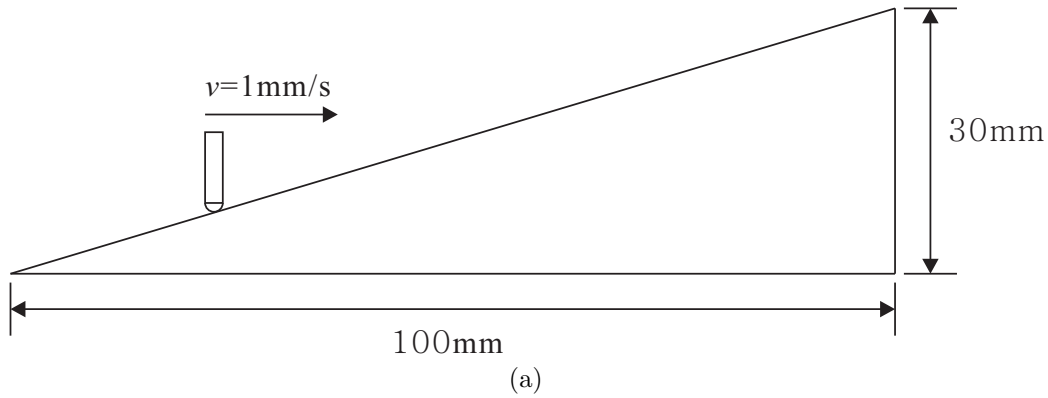


Figure 3.4: Experimental setup (a) and results (b) for smooth slope glass surface

3.5 (b), suggesting that the recorded data can approximately express the shape of curved surface.

Thirdly, sandpaper set MH913 of grit size #100, #320 and #1000 are selected as typical rough surfaces, as shown in Fig. 3.6 (a). The larger the grit size number, the smoother the sandpaper. For sandpaper of each grit size, the experiments are repeated 5 times. One instance of recorded data

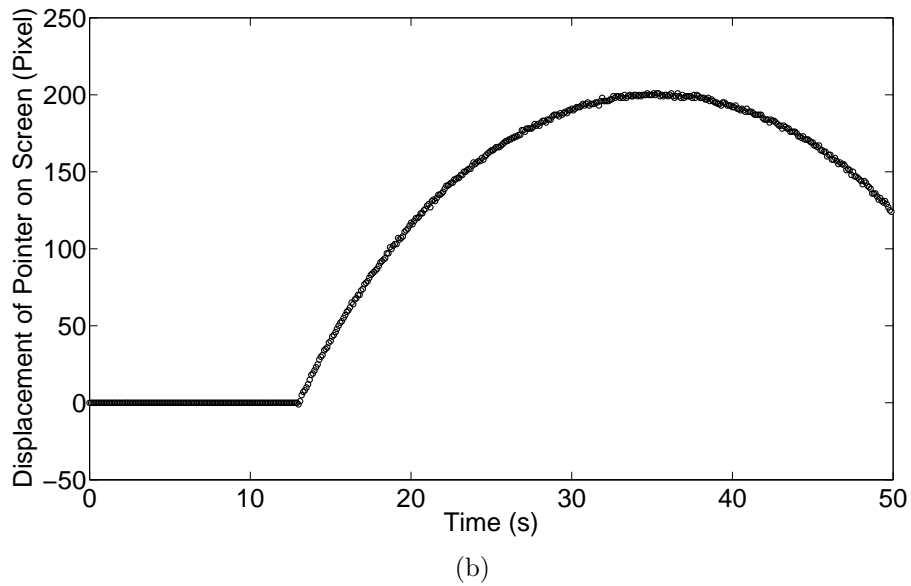
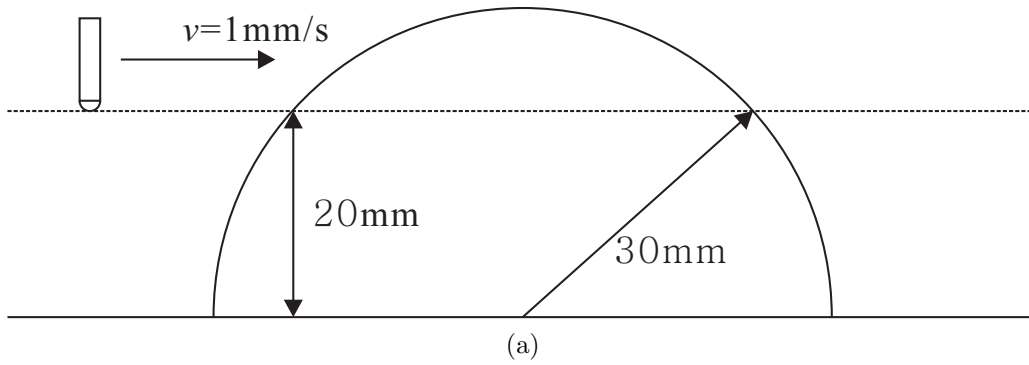


Figure 3.5: Experimental setup (a) and results (b) for smooth semi cylindrical acrylic surface. The device is at a height of 20mm to make the height variance of the object surface is in the maximum applicable surface height variance measurement range.

sequence responding to sandpaper of each grit size is shown in Fig. 3.6 (b) and the standard deviations of the all the 5 instances are shown in Table. 3.1. Confined by the minimum of detectable height variance, the proposed device can't track the detail of the sandpaper surfaces, but can estimate the roughness statistically. And the sandpaper of grit size #1000 is too smooth

to cause surface height variance more than the minimum of detectable height variance of the device.

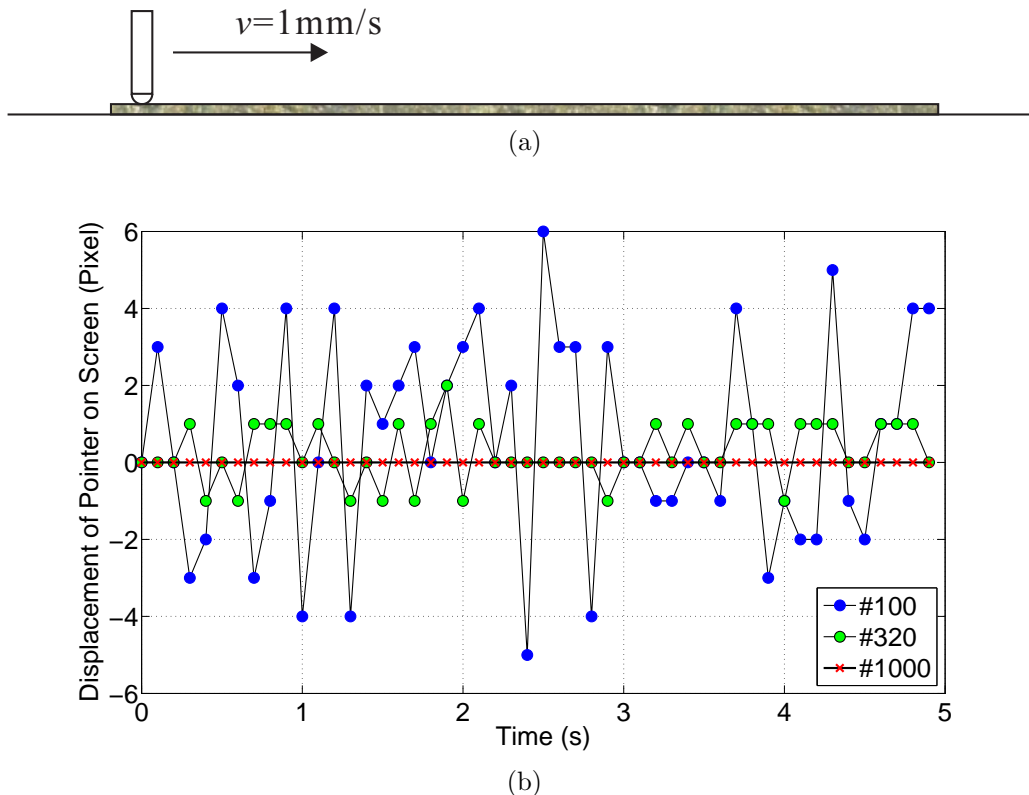


Figure 3.6: Experimental setup (a) and results (b) for sandpaper set MH913. Intuitively, the less the grit size number, the more dispersive the recorded data.

3.5 Conclusion

There are following advantages for the proposed device, and most of them are derived from the employment of the optical mouse sensor. The output of the system is digital, without the need of any additional analog-to-digital component. The interface is ready for use. The driver and software for the

Table 3.1: Standard deviations of experimental results for sandpaper set MH913

| | 1 | 2 | 3 | 4 | 5 |
|-------|--------|--------|--------|--------|--------|
| #100 | 2.6870 | 2.4126 | 2.5655 | 2.7367 | 2.7918 |
| #320 | 0.7508 | 0.7398 | 0.6893 | 0.7239 | 0.6987 |
| #1000 | 0.0000 | 0.1414 | 0.2020 | 0.0000 | 0.0000 |

sensing system is easily available. The outputs of the device can be intuitively displayed on the display and recorded on the hard disk, which greatly improves the convenience of the system. Because of the volume manufacture of the optical mouse sensor, the sensing system is cost-effective, and thus is easily available and generalized.

In summary, a device for analyzing the surface shape is reported, taking advantage of an optical mouse sensor. For smooth surface, the device can record the surface shape digitally, and for rough surface, the device can estimate the roughness in a statistical way. The resolution of the device is restricted by the resolution of the optical mouse sensor and the size of the ballpoint in the "antenna".

Chapter 4

Non-contact Tactile Sensing with Optical Mouse Sensor

4.1 Introduction

This chapter reviews the tactile sensing and then propose the primary idea of the non-contact tactile sensing with optical mouse sensor. Experiments on two groups of test objects are performed.

4.2 Tactile Sensing

Touch and tactile sensor are devices which measures the parameters of a contact between the sensor and an object. This interaction obtained is confined to a small defined region. This contrasts with a force and torque sensor that measures the total forces being applied to an object. In the consideration of tactile and touch sensing, the following definitions are commonly used:

Touch Sensing This is the detection and measurement of a contact force at a defined point. A touch sensor can also be restricted to binary information, namely touch, and no touch.

Tactile Sensing This is the detection and measurement of the spatial distribution of forces perpendicular to a predetermined sensory area, and the subsequent interpretation of the spatial information. A tactile-sensing array can be considered to be a coordinated group of touch sensors.

Slip This is the measurement and detection of the movement of an object relative to the sensor. This can be achieved either by a specially designed slip sensor or by the interpretation of the data from a touch sensor or a tactile array.

Tactile sensors can be used to sense a diverse range of stimulus ranging from detecting the presence or absence of a grasped object to a complete tactile image. A tactile sensor consists of an array of touch sensitive sites, the sites may be capable of measuring more than one property. The contact forces measured by a sensor are able to convey a large amount of information about the state of a grip. Texture, slip, impact and other contact conditions generate force and position signatures, that can be used to identify the state of a manipulation. This information can be determined by examination of the frequency domain, and is fully discussed in the literature.

As there is no comprehensive theory available that defines the sensing requirements for a robotic system, much of the knowledge is drawn from investigation of human sensing, and the analysis of grasping and manipulation. Study of the human sense of touch suggests that creating a gripper incorporating tactile sensing requires a wide range of sensors to fully determine the state of a grip. The detailed specification of a touch sensor will be a function of the actual task as it is required to perform. Currently no general specification of a touch or tactile sensor exists the following can be used as an excellent basis for defining the desirable characteristics of a touch or tactile sensor suitable for the majority of industrial applications:

1. A touch sensor should ideally be a single-point contact, through the sensory area can be any size. In practice, an area of 1-2 mm^2 is considered a satisfactory compromise between the difficulty of fabricating a sub-miniature sensing element and the coarseness of a large sensing element.
2. The sensitivity of the touch sensor is dependent on a number of variables determined by the sensor's basic physical characteristic. In addition the sensitivity may also be the application, in particular any physical barrier between the sensor and the object. A sensitivity within the range 0.4 to 10N, together with an allowance for accidental mechanical overload, is considered satisfactory for most industrial applications.
3. A minimum sensor bandwidth of 100 Hz.

4. The sensors characteristics must be stable and repeatable with low hysteresis. A linear response is not absolutely necessary, as information processing techniques can be used to compensate for any moderate non-linearities.
5. As the touch sensor will be used in an industrial application, it will need to be robust and protected from environmental damage.
6. If a tactile array is being considered, the majority of application can be undertaken by an array 10-20 sensors square, with a spatial resolution of 1-2 mm.

4.2.1 Touch Sensor Technology

Many physical principles have been exploited in the development of tactile sensors. As the technologies involved are very diverse, this chapter can only consider the generalities of the technology involved. In most cases, the developments in tactile sensing technologies are application driven. It should be recognized that the operation of a touch or tactile sensor is very dependant on the material of the object being gripped.. The sensors discussed in this chapter are capable of working with rigid objects. However if non-rigid material is being handled problems may arise. Work has shown that conventional sensors can be modified to operate with non-rigid materials.

Mechanically Based Sensors

The simplest form of touch sensor is one where the applied force is applied to a conventional mechanical micro-switch to form a binary touch sensor. The

force required to operate the switch will be determined by the its actuating characteristics and any external constraints. Other approaches are based on a mechanical movement activating a secondary device such as a potentiometer or displacement transducer.

Resistive Based Sensors

The use of compliant materials that have a defined force-resistance characteristics have received considerable attention in touch and tactile sensor research. The basic principle of this type of sensor is the measurement of the resistance of a conductive elastomer or foam between two points. The majority of the sensors use an elastomer that consists of a carbon doped rubber.

Force Sensing Resistor

A force sensing resistor is a piezoresistivity conductive polymer, which changes resistance in a predictable manner following application of force to its surface. It is normally supplied as a polymer sheet which has had the sensing film applied by screen printing. The sensing film consists of both electrically conducting and non-conducting particles suspended in matrix. The particle sizes are of the order of fraction of microns, and are formulated to reduce the temperature dependence, improve mechanical properties and increase surface durability. Applying a force to the surface of a the sensing film causes particles to touch the conducting electrodes, changing the resistance of the film. As with all resistive based sensors the force sensitive resistor requires a relatively simple interface and can operate satisfactorily in moderately hostile

environments.

Capacitive Based Sensors

A capacitive touch sensor relies on the applied force either changing the distance between the plates or the effective surface area of the capacitor. In such a sensor the two conductive plates of the sensor are separated by a dielectric medium, which is also used as the elastomer to give the sensor its force-to-capacitance characteristics.

To maximize the change in capacitance as force is applied, it is preferable to use a high permittivity, dielectric in a coaxial capacitor design. . In this type of sensor, as the size is reduced to increase the spatial resolution, the sensors absolute capacitance will decrease. With the limitations imposed by the sensitivity of the measurement techniques, and the increasing domination of stray capacitance, there is an effective limit on the resolution of a capacitive array. The figure shows the cross section of the capacitive touch transducer in which the movement of a one set of the capacitors' plates is used to resolve the displacement and hence applied force. The use of a highly dielectric polymer such as polyvinylidene fluoride maximizes the change capacitance. From an application viewpoint, the coaxial design is better as its capacitance will give a greater increase for an applied force than the parallel plate design.

To measure the change in capacitance, a number of techniques can be, the most popular is based on the use of a precision current source. A second approach is to use the sensor as part of a tuned or L.C. circuit, and measure the frequency response. Significant problem with capacitive sensors can be caused if they are in close proximity with the end effectors or robots earthed

metal structures, this leads to stray capacitance. This can be minimized by good circuit layout and mechanical design of the touch sensor. It is possible to fabricate a parallel plate capacitor on a single silicon slice, this can give a very compact sensing device.

Magnetic Based Sensor

There are two approaches to the design of touch or tactile sensors based on magnetic transduction. Firstly, the movement of a small magnet by an applied force will cause the flux density at the point of measurement to change. The flux measurement can be made by either a Hall effect or a magnetoresistive device. Second, the core of the transformer or inductor can be manufactured from a magnetoelastic material that will deform under pressure and cause the magnetic coupling between transformer windings, or a coils inductance to change. A magnetoresistive or magnetoelastic material is a material whose magnetic characteristics are modified when the material is subjected to changes in externally applied physical forces. The magnetorestrictive or magnetoelastic sensor has a number of advantages that include high sensitivity and dynamic range, no measurable mechanical hysteresis, a linear response, and physical robustness.

If a very small permanent magnet is held above the detection device by a compliant medium, the change in flux caused by the magnet's movement due to an applied force can be detected and measured. The field intensity follows an inverse relationship, leading to a nonlinear response, which can be easily linearized by processing. A one-dimensional sensor where a row of twenty hall effect devices placed opposite a magnet has been constructed. A tactile

sensor using magnetoelastic material has been developed, where the material was bonded to a substrate, and then used as a core for an inductor. As the core is stressed, the materials susceptibility changed, which is measured as a change in the coils inductance.

Optical Sensors

The rapid expansion of optical technology in recent years has led to the development of a wide range of tactile sensors. The operating principles of optical-based sensors are well known and fall into two classes:

1. *Intrinsic*, where the optical phase, intensity, or polarization of transmitted light are modulated without interrupting the optical path
2. *Extrinsic*, where the physical stimulus interacts with the light external to the primary light path.

Intrinsic and extrinsic optical sensors can be used for touch, torque, and force sensing. For industrial applications, the most suitable will be that which requires the least optical processing. For example the detection of phase shift, using interferometry, is not considered a practical option for robotic touch and force sensors. For robotic touch and force-sensing applications, the extrinsic sensor based on intensity measurement is the most widely used due to its simplicity of construction and the subsequent information processing. The potential benefits of using optical sensors can be summarized as follow:

Immunity to external electromagnetic interference, which is widespread in robotic applications.

1. Intrinsically safe.

2. The use of optical fibre allows the sensor to be located some distance from the optical source and receiver.
3. Low weight and volume.

Touch and tactile optical sensors have been developed using a range of optical technologies:(a) Modulating the intensity of light by moving an obstruction into the light path.(b) Photoelasticity.

Optical Fibre Based Sensors

Tactile sensors can be constructed from the fibre itself. A number of tactile sensors have been developed using this approach. In the majority of cases either the sensor structure was too big to be attached to the fingers of robotic hand or the operation was too complex for use in the industrial environment. A suitable design can be based on internal-state microbending of optical fibres. Microbending is the process of light attenuation in the core of fibre when a mechanical bend or perturbation (of the order of few microns) is applied to the outer surface of the fibre. The degree of attenuation depends on the fibre parameters as well as radius of curvature and spatial wavelength of the bend. Research has demonstrate the feasibility of effecting microbending on an optical fibre by the application of a force to a second orthogonal optical fibre.

Piezoelectric Sensors

Polymeric materials that exhibit piezoelectric properties are suitable for use as a touch or tactile sensors, while quartz and some ceramics have piezoelec-

tric properties, polymers such as polyvinylidene fluoride (PVDF) are normally used in sensors.

Polyvinylidene fluoride is not piezoelectric in its raw state, but can be made piezoelectric by heating the PVDF within an electric field. Polyvinylidene fluoride is supplied sheets between as 5 microns and 2 mm thick, and has good mechanical properties. A thin layer of metalization is applied to both sides of the sheet to collect the charge and permit electrical connections being made. In addition it can be moulded, hence PVDF has number of attraction when considering tactile sensor material as an artificial skin.

Strain Gauges in Tactile Sensors

A strain gauge when attached to a surface will detect the change in length of the material as it is subjected to external forces. The strain gauge is manufactured from either resistive elements (foil, wire, or resistive ink) or from semiconducting material. A typical resistive gauge consists of the resistive grid being bonded to an epoxy backing film. If the strain gauge is pre-stressed prior to the application of the backing medium, it is possible to measure both tensile and compressive stresses. The semi-conducting strain gauge is fabricated from a suitable doped piece of silicone, in this case the mechanism used for the resistance change is the piezoresistive effect.

When applied to robotic touch applications, the strain gauge is normally used in two configurations: as a load cell, where the stress is measured directly at the point of contact, or with the strain gauge positioned within the structure of the end effector.

Silicon Based Sensors

Technologies for micromachining sensors are currently being developed worldwide. The developments can be directly linked to the advanced processing capabilities of the integrated circuit industry, that has developed fabrication techniques that allow the interfacing of the non-electronic environment to be integrated through micro-electromechanical systems.. Though not as dimensionally rigorous as the more mature silicon planer technology, micromachining is inherently more complex as it involves the manufacture of a three-dimensional object. Therefore the fabrication relies on additive layer techniques to produce the mechanical structure.

The excellent characteristics of silicon, that has made micromachined sensors possible, include a tensile strength comparable to steel, elastic to breaking point, and there is very little mechanical hysteresis in devices made from a single crystal, a low thermal coefficient of expansion.

To date it is apparent that microengineering has been applied most successfully to sensors. Some sensor applications take advantage of the device-to-device or batch-to-batch repeatability of wafer-scale processing to remove expensive calibration procedures. Current applications are restricted largely to pressure and acceleration sensors, though these in principle can be used as force sensors. As the structure is very delicate, there still are problems in developing a suitable tactile sensor for industrial applications.

Smart Sensors

The most significant problem with the sensor systems discussed so far is that of signal processing. Researchers are therefore looking to develop a complete sensing system rather than individual sensors, together with individual interfaces and interconnections. This allows the signal processing to be brought as close as possible to the sensor itself or integrated with the sensor. Such sensors are generally termed smart sensors. It is the advances in silicon fabrication techniques which have enabled the recent developments in smart sensors. There is no single definition of what a smart sensor should be capable of doing, mainly because interest in smart sensors is relatively new. However, there is a strong feeling that the minimum requirements are that the sensing system should be capable of self diagnostics, calibration and testing. As silicon can be machined to form moving parts such as diaphragms and beams, a tactile sensor can in principal be fabricated on single piece of silicon. Very little commercial success has been obtained so far, largely due to the problems encountered in transferring the technology involved from the research laboratory to industry. In all tactile sensors their is a major problem of information processing, and interconnection. An array has $2n$ connection and individual wires, any reduction in interconnection requirements is welcomed due to ease of construction and increased reliability. A number of researchers have been addressing the problem of integrating a tactile sensor with integral signal processing. In this design the sensors conductive elastomer sheet was placed over a substrate. The significant feature of this design is that the substrate incorporated VLSI circuitry so that each sensing element not only

measures its data but processes it as well. Each site performs the measurements and processing operations in parallel. The main difficulty with this approach was the poor discrimination, and susceptibility to physical damage. However, the VLSI approach was demonstrated to be viable, and alleviated the problems of wiring up each site and processing the data serially.

Multi-stimuli Touch Sensors

It has been assumed that all the touch sensors discussed in this section respond only to a force stimulus. However, in practice most respond to other external stimuli, in particular, temperature. If PVDF has to be used as a force sensor in an environment with a widely varying ambient temperature, there may be a requirement for a piece of unstressed PVDF to act as a temperature reference. It is possible for a sensor to respond both to force and temperature changes. This has a particular use for object recognition between materials that have different thermal conductivity, e.g., between a metal and a polymer. If the complexity of the interpretation of data from PVDF is unsuitable for an application, touch sensors incorporating a resistive elastomer for force, and thermistors for temperature measurement can be constructed. By the use of two or more force-sensitive layers on the sensor, which have different characteristics (e.g., resistive elastomer and PVDF), it is possible to simulate the epidermal and dermal layers of human skin.

4.3 Primary Idea for Non-contact Tactile Sensing

One of the important performance specifications of an optical mouse sensor is the resolution. Resolution reflects the number of steps the optical mouse sensor will report when it moves one inch, expressed in dpi (dots-per-inch).

Practically, if an optical mouse sensor is in a uniform motion for a constant time, the displacement of the pointer on the display is proportional to the resolution of the optical mouse sensor, and thus the displacement of the pointer on the display can be employed as a measure of the resolution.

Fig. 4.1 shows the distance from lens reference plane to surface, denoted as z .

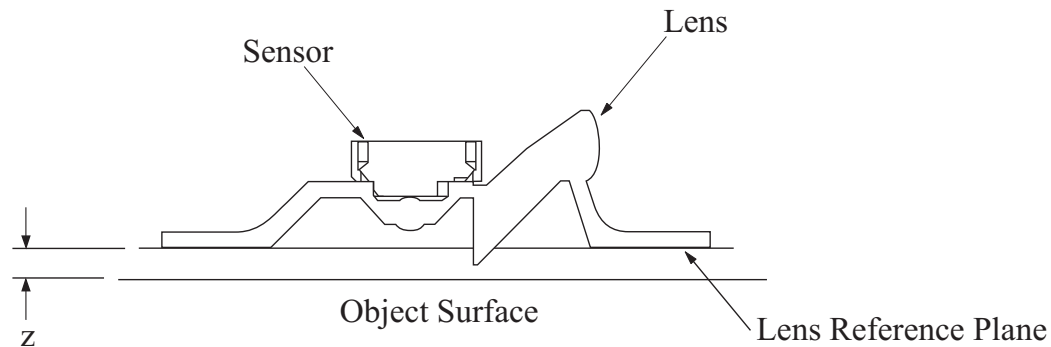


Figure 4.1: Distance from lens reference plane to surface

In recommended operating condition for the optical mouse sensor, the minimum of z is 2.3mm, the maximum of z is 2.5mm, and the typical of z is 2.4mm. In normal cases, the object surface is flat, and the distance between the optical mouse sensor and the object surface is constant.

Intuitively, during the daily use, if an optical mouse is lifted away from

the working surface and the height from the optical mouse to the working surface is above some value, the resolution of the optical mouse decreases to zero. It can be seen that the resolution of an optical mouse sensor is related to the height from the optical mouse to the working surface. It is an interesting idea to make an optical mouse sensor work in the manner of human hand but in a non-contact way to "feel" the object surface based on the characteristics mentioned above.

If the object surface is not flat, when the optical mouse sensor is moved horizontally, z is variable, a variable resolution will show, which will influence the pointer motion on the computer screen. So analyzing the pointer track on the screen can provide some information of the shape of the object surface.

Based on the ideas mentioned above, in following experiments, firstly, two rubber surfaces with regular surface shapes are prepared, an optical mouse sensor which is placed over the object surfaces is controlled by a robot arm, and a MATLAB application is developed to record the pointer motion on the computer screen; and secondly, whitepaper is used as the test object in the same experiment procedures.

4.4 Experiment Setup

The diagram of the experiment system is shown in Fig. 4.2.

The relative coordinate system is shown as Fig. 4.3.

The x - y coordinate system is the coordinate system for the object surface and the a - b coordinate system is the coordinate system for the optical mouse sensor. Here, α is a variable angle between a -axis and x -axis.

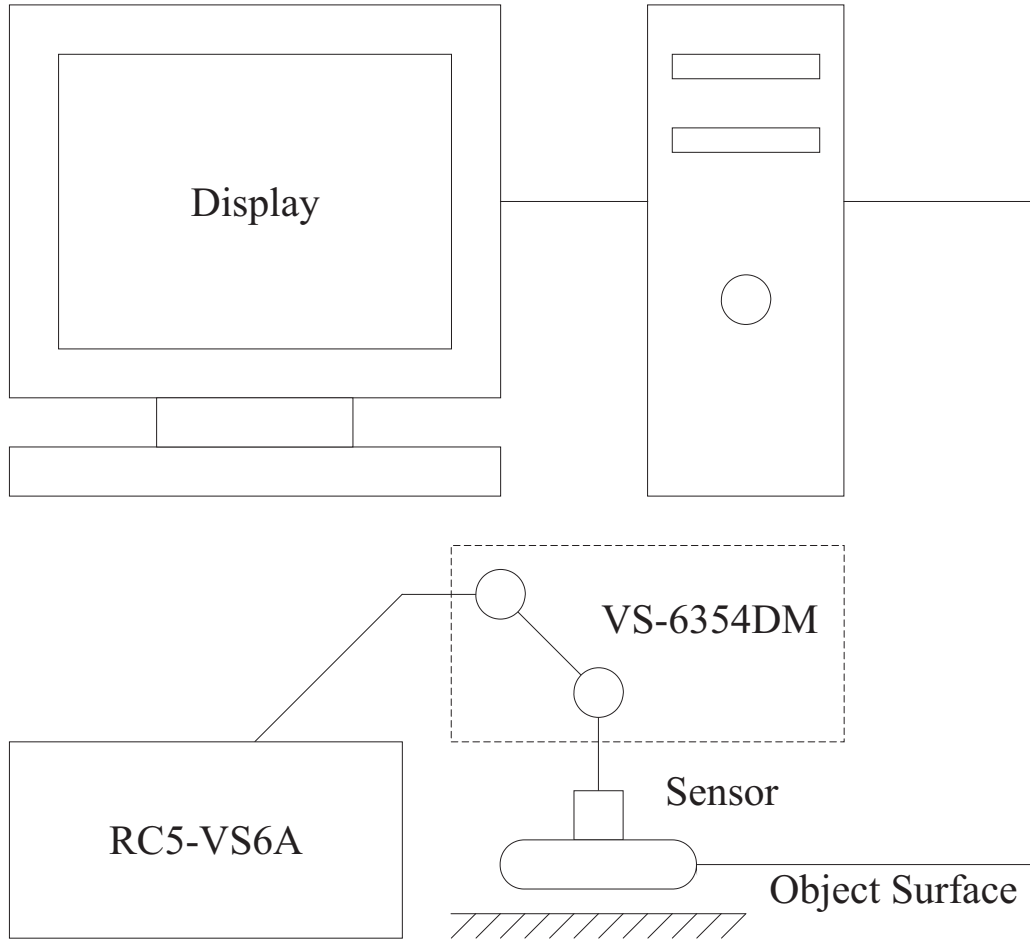


Figure 4.2: Diagram of the experiment system for non-contact tactile sensing

A robot arm of model VS-6354DM is controlled by a robot controller of model RC5-VS6A. Both of VS-6354DM and RC5-VS6A are manufactured by DENSO Corporation. In each of X, Y, and Z directions, the position repeatability of the robot arm of model VS-6354DM is ± 0.02 mm.

The optical mouse sensor used for the experiment is from an optical mouse manufactured by Logitech, and the product number is SOM-U20. The part number of the optical mouse sensor is S2599, which is manufactured by Agilent Technologies. The nominated resolution of S2599 is 400dpi.

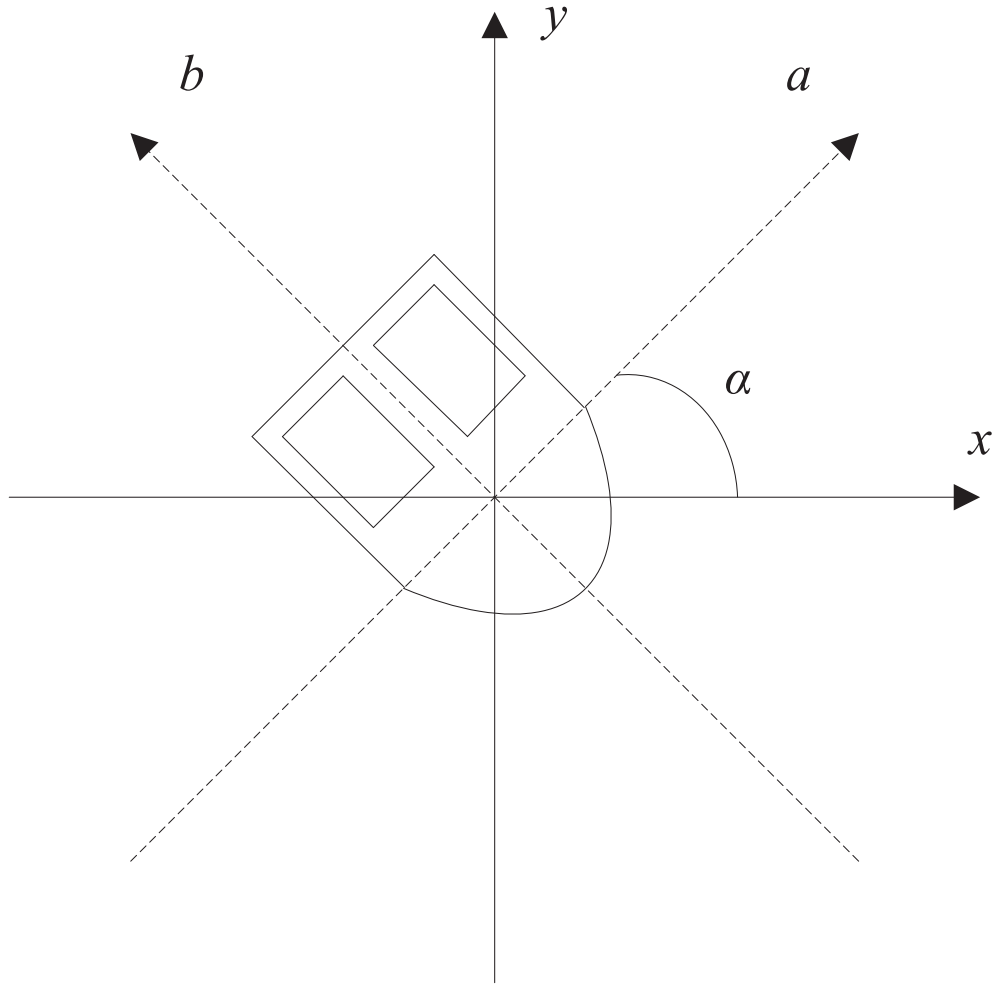


Figure 4.3: Sensing coordinate systems for non-contact tactile sensing

In the Windows XP operating system, the pointer speed is set to the fastest and the property "Enhance pointer precision" is enabled, which help improve the system sensitivity, as shown in Fig. 4.4.

The output of the sensing system is a sequence (x_i, y_i) , which describes the track of the pointer on the computer screen. Index i is integers in the interval $[1, 1000]$, x is in the interval $[1, 1024]$ and y is in the interval $[1, 768]$.



Figure 4.4: System configuration of mouse in the experiments

4.5 Experiment on Rubber Surfaces

The sensing objects are two rubber surfaces. Two object surfaces with different surface shapes are prepared, that is the periodically-square-shaped rubber surface and the periodically-arc-shaped rubber surface. The 3-D view of the two object surfaces are shown in Fig. 4.5.

In order to get the characteristics of resolution vs. height for the rubber surface used in the experiments, z is changed from 1.4mm to 2.8mm by a step of 0.2mm and α is changed from 0° to 90° by a step of 30° . The translation velocity of the robot arm is set as 1mm/s, and the translation time is 10s. For the uniform translation, the displacement of pointer on the screen is proportional to the resolution of the optical mouse sensor. The characteristics of resolution vs. height are shown in Fig. 4.6. It can be seen that the characteristics are monotonic in the interval [1.4mm, 2.8mm], and surface height variation of 0.2mm can be measured.

4.5.1 Tests on the Two Rubber Surfaces

In the tests, the sampling interval is 0.05s and each group of data includes 1000 points, so the total sampling time for each group is 50s.

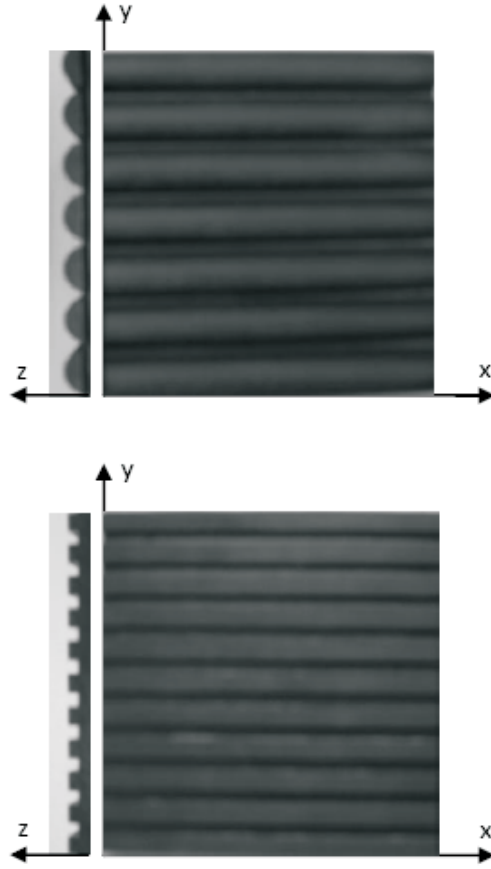


Figure 4.5: 3-D view of the two rubber surfaces used for non-contact tactile sensing

Firstly, the periodically-square-shaped surface is placed under the optical mouse sensor, and α is set as 0° . Then the optical mouse sensor is moved over the object surface at a uniform speed of 1mm/s in the y -axis direction controlled by the robot arm VS-6354DM, while the MATLAB application records the pointer positions on the screen. The angle between a -axis and x -axis α is changed from 0° to 90° by a step value of 10° , and the above procedures are repeated.

Secondly, procedures above are repeated on the periodically-arc-shaped

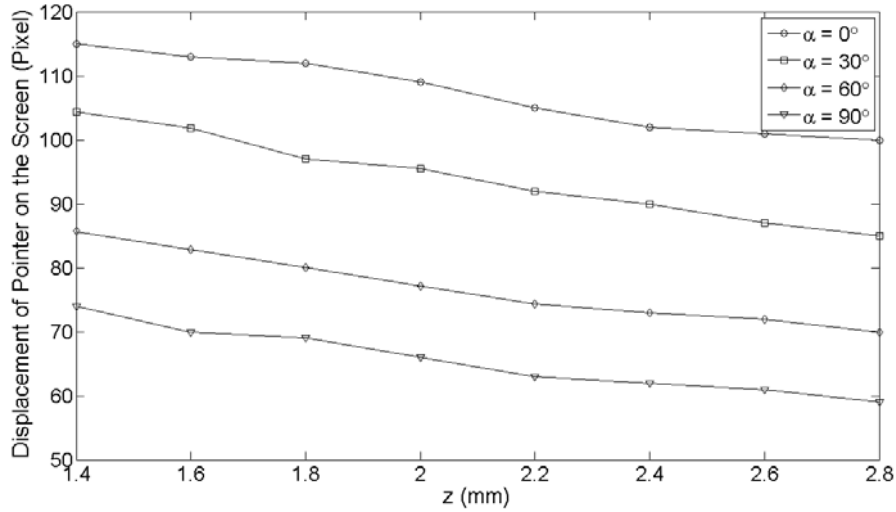


Figure 4.6: Characteristics of resolution vs. height for the rubber surface surface.

Finally, 20 track curves of the pointer on the screen are obtained.

In order to simplify the data processing, the starting point of each track curve coordinates is translated to $(0, 0)$, because it is the relative displacement that makes sense. In order to simplify the explanation, 6 typical track curves are employed.

4.5.2 Translation Direction Measurement

In the experiments, the object surfaces are fixed, and the obtained direction is the direction of the translation of the optical mouse sensor, as shown in Fig. 4.7 and Fig. 4.8.

The former is obtained when the object surface is periodically-square-shaped, and the later is obtained when the object surface is periodically-arc-shaped.

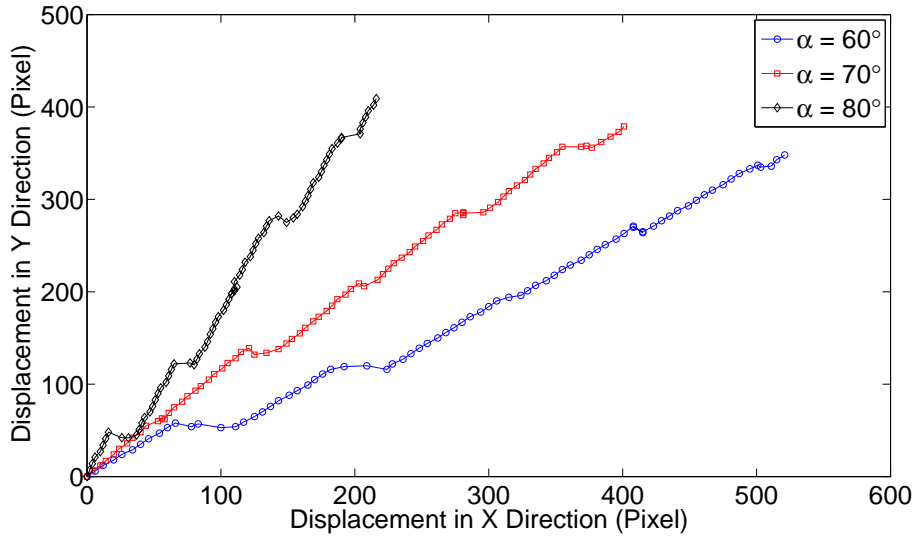


Figure 4.7: Track curves of different directions for periodically-square-shaped surface

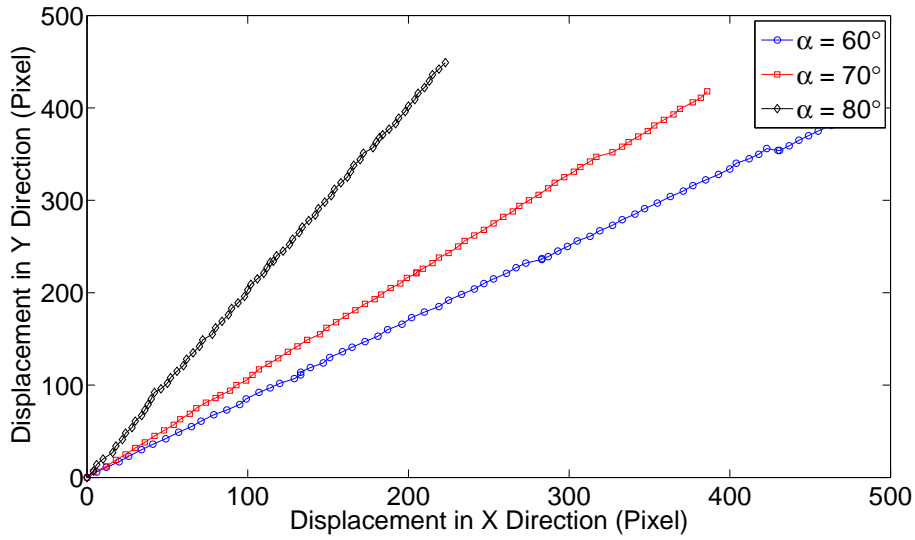


Figure 4.8: Track curves of different directions for periodically-arc-shaped surface

From the point of relative movement, the translation direction of the surface and the direction of the surface textures can be obtained, as shown

in Fig. 4.9 and Fig. 4.10. The slope of the linear part reveals the angle.

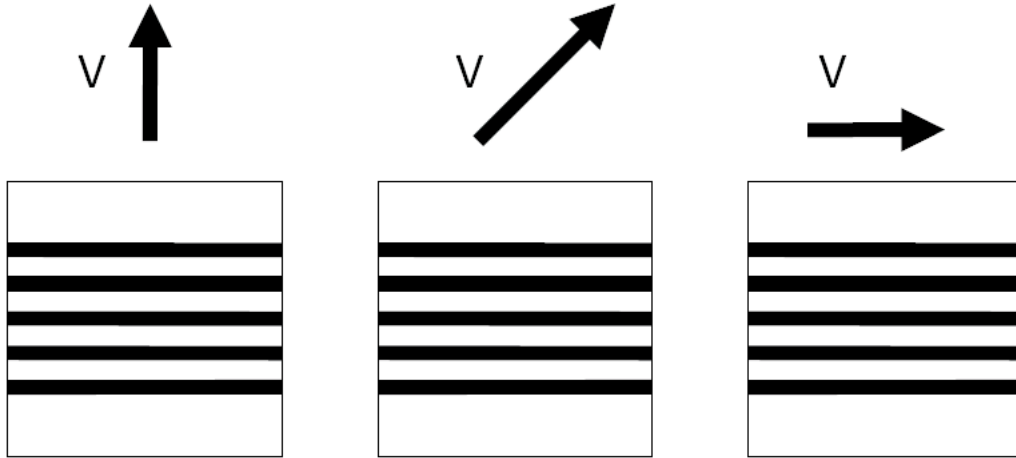


Figure 4.9: Different translation directions in non-contact tactile sensing

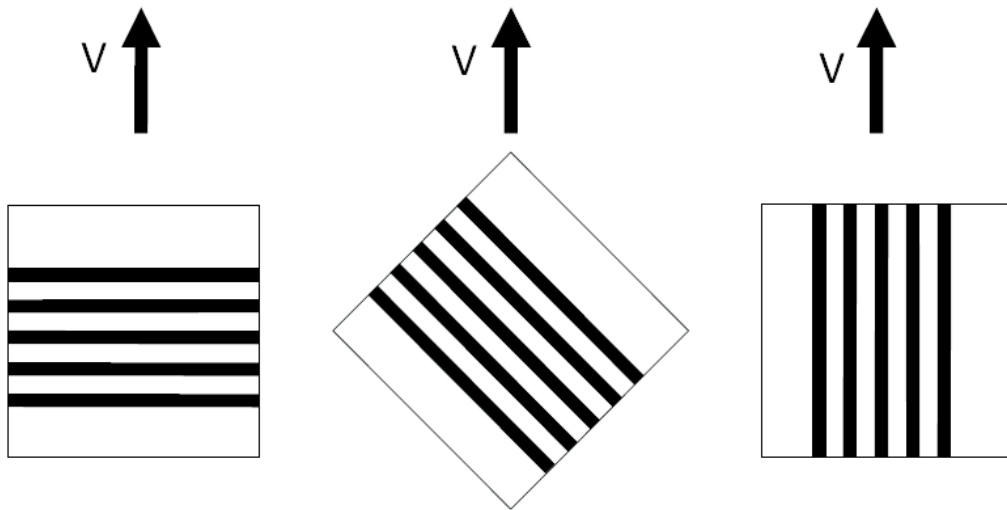


Figure 4.10: Different texture directions in non-contact tactile sensing

During the experiment, it is found that the a -axis sensitivity and b -axis sensitivity of the optical mouse sensor are different. For example, in the case of $\alpha = 70^\circ$, in Fig. 4.11, if the a -axis sensitivity and b -axis sensitivity of the optical mouse sensor are the same, the track curve for $\alpha = 70^\circ$ and the curve

of $y/x = \arctan(70^\circ)$ will be of the same slope. It can be seen that a -axis sensitivity is less than b -axis sensitivity. This is because the illumination of the LED is from the side, not vertically and symmetrically.

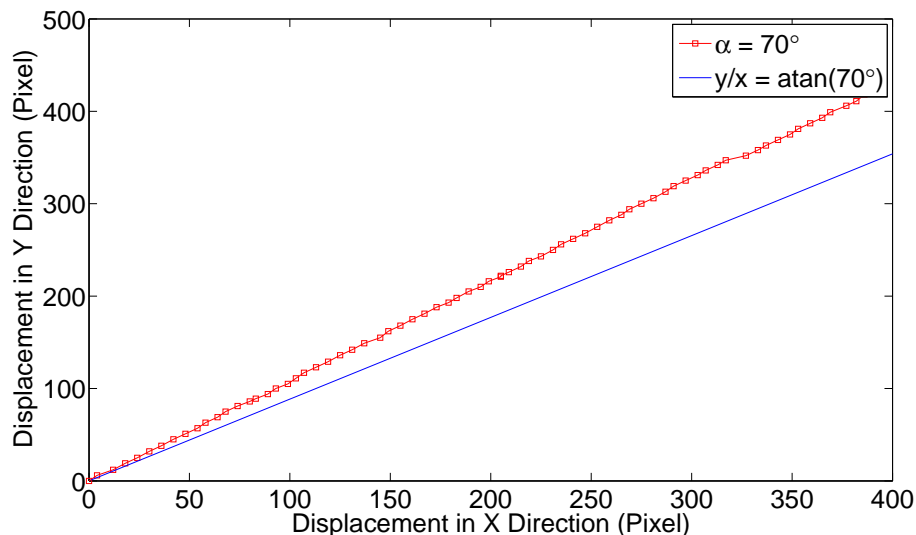


Figure 4.11: a -axis and b -axis of different resolutions ($\alpha = 70^\circ$)

4.5.3 The Surface Shape of the Object Surface

The surface height is one kind of description of the surface shape. If the height variation range of the object surface is less than the range of the monotonic interval of the characteristics of resolution vs. height, by setting the initial distance between the lens reference plane and object surface properly, the height variation interval of the object surface can fall in the monotonic interval. When the optical mouse sensor is moved over the object surface at a uniform speed, for a fixed direction, the slope of the track curve of the pointer on the screen is a measure of the surface height. When the surface height is the same, the slope of the track curve is the same. In Fig. 4.7 and

Fig. 4.8, the periodically-square-shaped rubber surface and the periodically-arc-shaped rubber surface are used to illustrate the fact qualitatively.

4.6 Experiments on Whitepaper

4.6.1 Experiments Procedures

Avago Technologies provides a computer application named "Cursor Tester" for the mouse bench test. Before the experiments, "Cursor Tester" is employed for direction calibration and parallelism calibration. The initial position and initial pose of the optical mouse sensor are adjusted by the robot arm while the outputs of "Cursor Tester" are observed and analyzed. After several recurrences of calibration, when $\alpha = 0^\circ$, if the optical mouse sensor is moved in the x -axis direction, there is zero displacement in the vertical axis direction on the display; if the optical mouse sensor is moved in the y -axis direction, there is zero displacement in the horizontal axis direction on the display; and the lens reference plane is parallel to the object surface.

In the experiments, for a given z and a given α initially set by the robot arm, the optical mouse sensor is moved over the object surface at a uniform velocity of 1mm/s and in the y -axis direction, the pointer position on the display varies and the pointer position is recorded by the MATLAB application.

In the MATLAB application, the sampling interval is set as 0.05s and the sampling length is set as 100, so the total sampling time for each data group is 5s. The output of the sensing system is a sequence (x_i, y_i) , which

describes the track of the pointer on the computer display and the length of the sequence is 100. x_i is in the interval $[1, 1024]$ and y_i is in the interval $[1, 768]$.

In order to simplify data processing, the starting point of each pointer track curve coordinates is translated to $(0, 0)$, because it is the relative displacement that makes sense.

For RHQ-100, $z = [1.6, 1.8, 2.0, 2.2, 2.4, 2.6, 2.8, 3.0, 3.2]$ mm, and $\alpha = [0, 10, 20, 30, 40, 50, 60, 70, 80, 90]$ °. Finally, 90 sequences of dimension 100×2 are obtained.

4.6.2 Translation Direction Measurement

The 1st dimension and 2nd dimension of the data table, that is (x_i, y_i) , are employed to calculate α . One estimate of $\tan()$ is the solution in the least squares sense to the overdetermined system of equations $\mathbf{Y}_{100 \times 1} \tan(\alpha') = \mathbf{X}_{100 \times 1}$. For calculation of each $\tan(\alpha')$, the average of 9 solutions of equations corresponding to 9 values of z are used. The relation between the estimated angle α' and the actual angle α is shown in Fig. 4.12. It can be seen that α' and α is not linearly related and a cubic polynomial provides a good fitting. That is, the angle α' presented on the display is not linearly related to the angle α set by the robot arm.

Furthermore, it can be concluded that the a-axis resolution and b-axis resolution of the optical mouse sensor are different. This is because the illumination of the LED is from the side, not vertically and symmetrically. Hereafter, the default resolution is referred to the b-axis resolution.

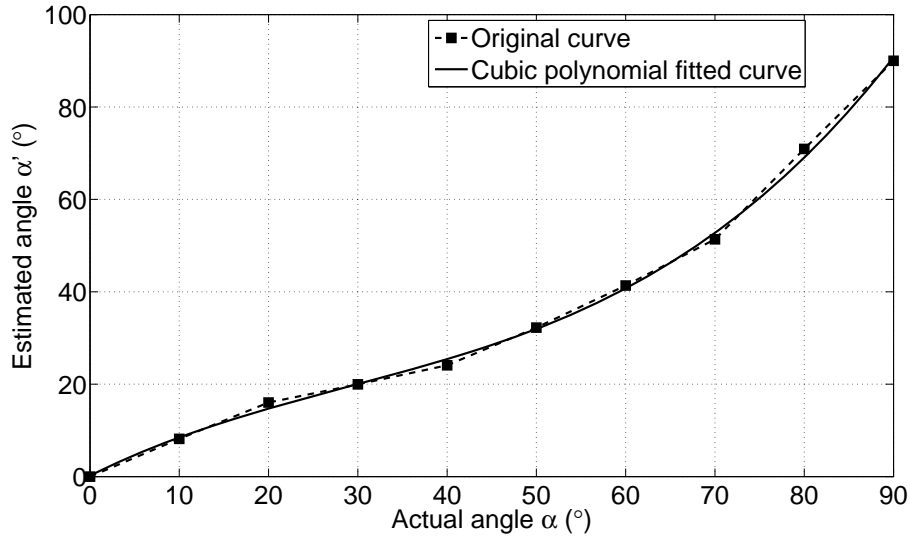


Figure 4.12: The relation between the estimated angle α' and the actual angle α .

4.6.3 Height Measurement

Based on the data table with $\alpha = 0^\circ$, the characteristics of resolution vs. height of whitepaper RHQ-100 is obtained, as shown in Fig. 4.13. In the interval [1.6, 2.2] mm, the characteristics curve is monotonically increasing, and in the interval [2.2, 3.2] mm, the characteristics curve is monotonically decreasing.

In the characteristics of resolution vs. height of an object surface, if the height variation range of the object surface is less than the range of a monotonic interval of the characteristics of resolution vs. height, by setting the initial height between the lens reference plane and the object surface properly, the height variation interval of the object surface can fall into the monotonic interval. In such a condition, the characteristics of resolution vs. height can be used for height measurement effectively. It can be seen that

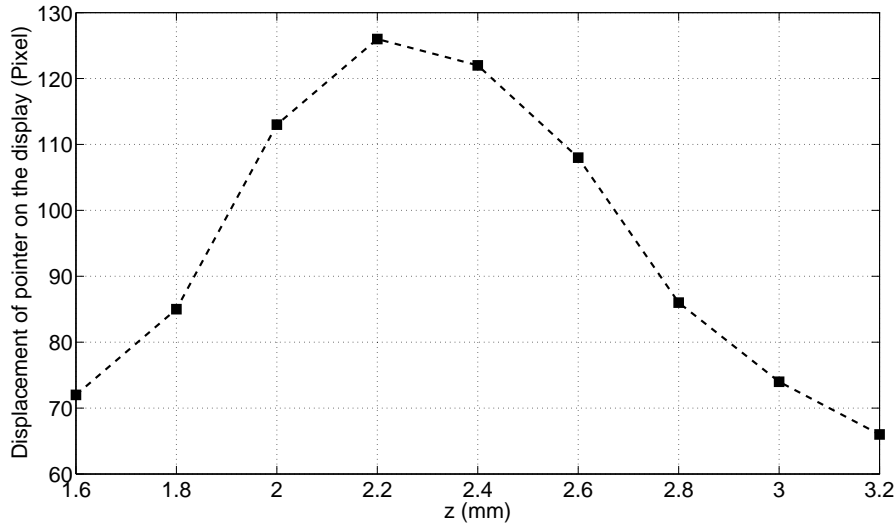


Figure 4.13: The characteristics of resolution vs. height of whitepaper RHQ-100.

height variation of 0.2mm can be detected.

For different object surface, the position and range of the monotonic interval of the characteristics of resolution vs. height are different.

4.6.4 Crack Detection

Based the feasibility of height measurement of an optical mouse sensor, it can be used for crack detection on a plane surface.

An object surface with specific crack configuration is constructed using whitepaper RHQ-100 as shown in Fig. 4.14. The zero reference height is $z = 3.2$ mm. The thickness of 2 pieces of whitepaper is about 0.2 mm. The thickness of the crackless object surface is of 4 pieces of whitepaper, the thickness of interval $[5, 7.5]$ mm is of 2 pieces of whitepaper, and the thickness of interval $[12.5, 17.5]$ mm is of 8 pieces of whitepaper.

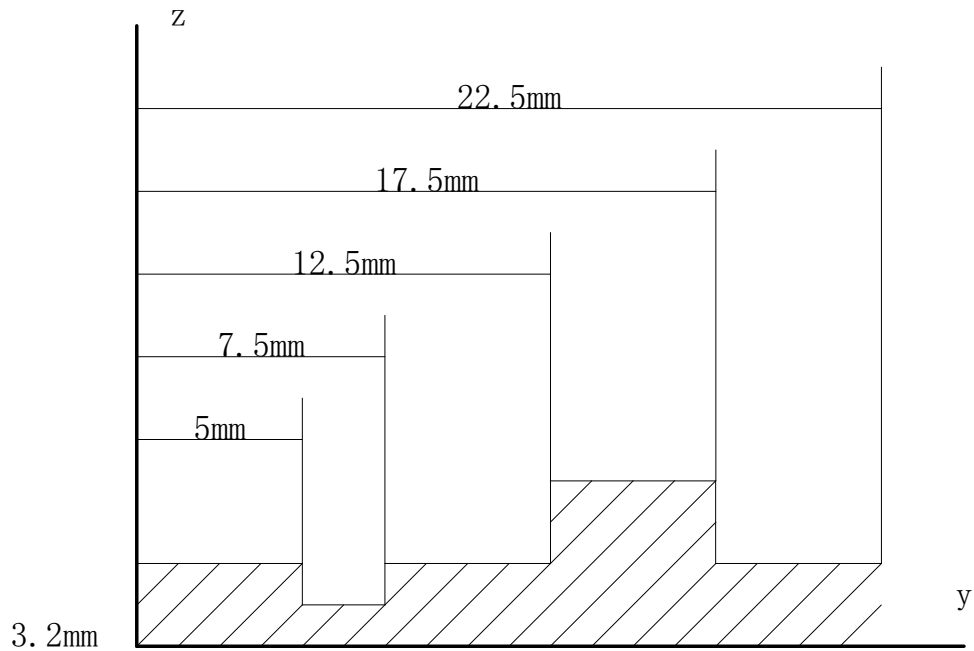


Figure 4.14: An object surface with specific crack configuration.

When $\alpha = 0^\circ$, the optical mouse sensor is moved over the constructed object surface at a uniform velocity of 1mm/s, and the pointer position on the display is recorded by the MATLAB application with a sampling interval of 0.05s. The position of the pointer on the display varies with the position of the optical mouse sensor in the y-axis direction, as shown in Fig. 4.15 with piecewise linear fitting. The solid lines correspond to the crackless parts, while the dashed lines correspond to the cracked parts.

A forward difference operation is performed on the curve in Fig. 4.15, and the result curve is shown in Fig. 4.16.

When the optical mouse sensor is moved over the object surface at a uniform velocity, the slope of the displacement curve of the pointer on the display is a measure of the surface height. When the surface heights are the

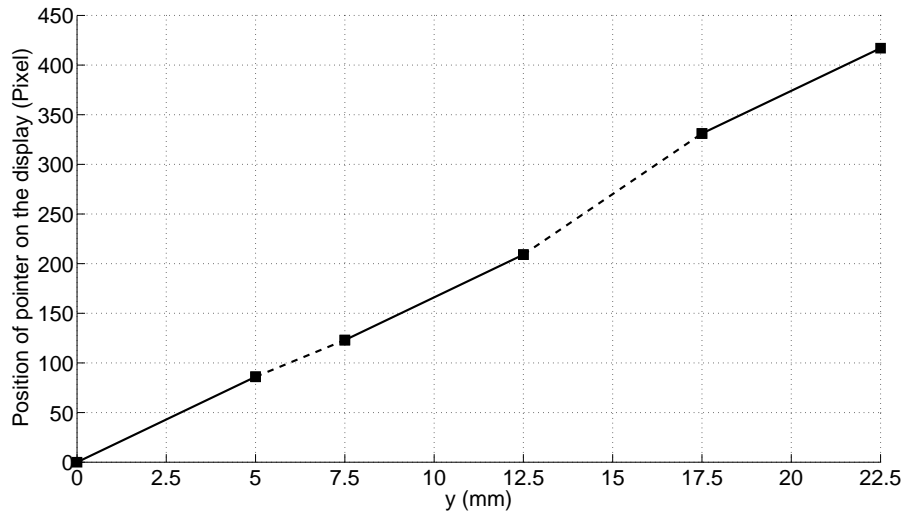


Figure 4.15: The position of the pointer on the display varies with the position of the optical mouse sensor in the y-axis direction.

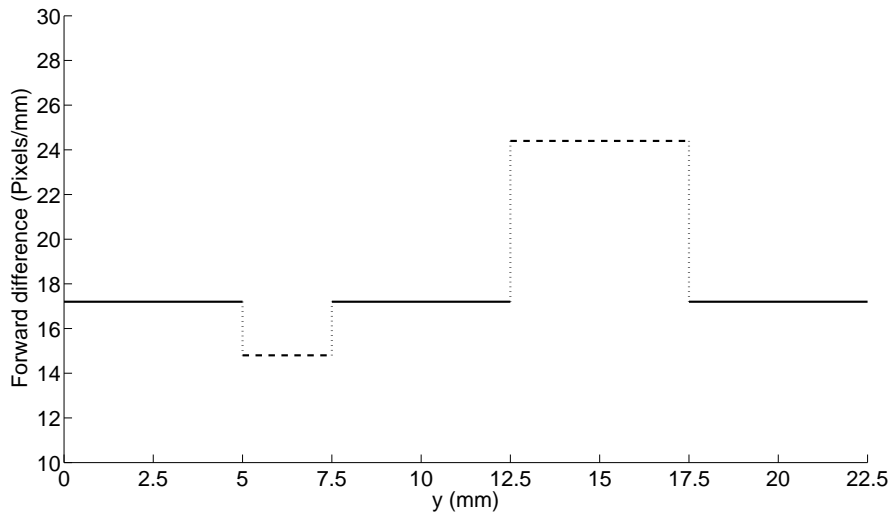


Figure 4.16: A forward difference operation is performed on the curve in Fig. 4.15.

same, the slopes of the corresponding displacement curve are the same.

4.6.5 Category Discrimination

As a human hand touches different object surfaces, the human feel is slightly different, and an optical mouse sensor can also feel the differences in a non-contact way based on the characteristics of resolution vs. height of different object surfaces. In such a case, the sensed surface differences are mainly roughness differences.

Fig. 4.17 is from a datasheet from Agilent Technologies. Burl Formica, white paper, manila, black copy and black walnut are standard surfaces which Agilent Technologies recommends to be used for surface navigation testing.

If the height from lens reference plane to object surface is selected properly, the surface discrimination can be performed based on the resolution differences at a specific height.

For each object surface, the characteristics of resolution vs. height are specific, and a specific characteristics curve can be selected by a specific curve segment. If the height from lens reference plane to object surface is unknown, in order to recognize a specific characteristics curve, two optical mouse sensors can cooperate, with a calibrated height difference (e.g. 0.2 mm) between the two optical mouse sensors. By matching the output of the two optical mouse sensors, a specific characteristics curve can be selected, and therefore the category of the object surface can be felt.

The characteristic of resolution vs. height of white paper in Fig. 4.17 differ much from that in Fig. 4.13. According to Application Note 5274 "Optical Navigation - Standard Surface Kit" from Agilent, the part number of the white paper they tested is OCE 8650000042 different from RHQ-100.

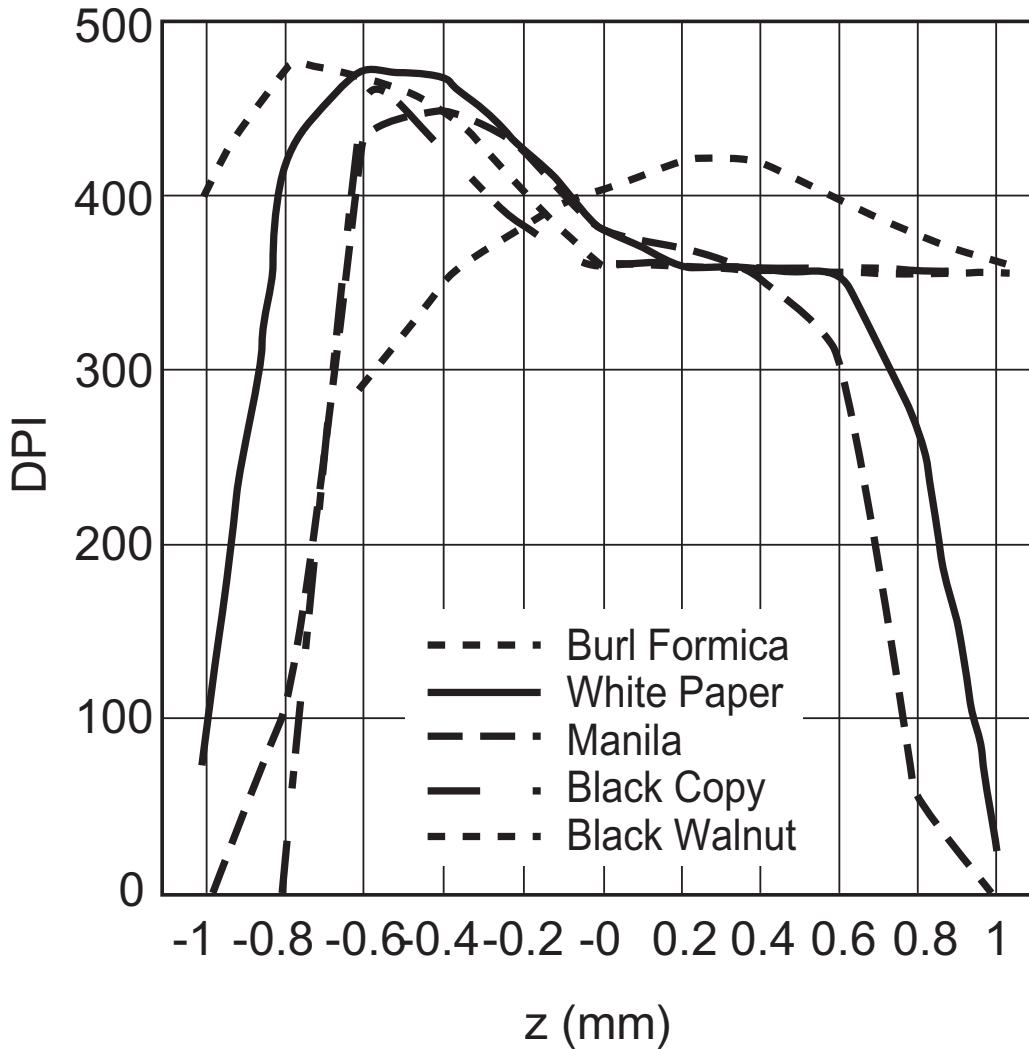


Figure 4.17: Burl Formica, white paper, manila, black copy and black walnut are standard surfaces which Agilent Technologies recommends to be used for surface navigation testing.

4.7 Discussion

In the experiments above, x is in the interval $[1, 1024]$ and y is in the interval $[1, 768]$. In actual applications, there may be some cases where x and y are beyond ranges above. In fact, this is a limitation caused by the driver software of the computer mouse. In actual applications, the direct output

signals of the optical mouse sensor, which is a two-channel quadrature output, can be used for processing. In such a way, without the intervention of the operating system and the driver, higher sensitivity and higher measurement speed can be expected. Furthermore, the two-channel quadrature output can be transformed by logic circuits to be used for PWM (Pulse Width Modulation) control in some industry applications.

In the experiments above, the nominated resolution of the employed optical mouse sensor is 400dpi. In the mainstream market, the resolution of an optical mouse sensor is 800dpi or higher. If higher sensitivity is required, an optical mouse sensor of higher resolution can be employed.

Position jitter is one of the noise sources of the measurement. Position jitter is an undesirable false movement of the pointer when an optical mouse is static. Such movements are usually small and can be seen on the display as jittering or even quivering. In our experiments, such an effect is superposed on the expected movement of the optical mouse sensor, and has been canceled by averaging and fitting.

As for the application of crack detection, real-time on-line detection can be expected by developing a novel detection algorithm.

In order to simplify the experiment setup and show the resolution of the system intuitively, we used the whitepaper as the test object. Practically, we can study the characteristics of resolution vs. height on each applicable surface to design a crack detection system for it.

Besides the height from lens reference plane to object surface and the category of the object surface, many other factors, such as the velocity of the sensor, LED current level and the wavelength responsibility of the LED,

influence the resolution and the output of the optical mouse sensor. In our current research, these parameters are constant, and the effects of them will be studied in further research work.

Besides the LED-based optical mouse sensor, the laser optical mouse sensor with superior performance is gradually popularized. The laser optical mouse sensor is enabled with Agilent's LaserStream Technology. LaserStream navigation engines provide much finer precision and more accurate tracking on a wider variety of surfaces, part of which proves difficult for traditional LED-based optical navigation, such as glossy and reflective surfaces. The adoption of the LaserStream Technology will help improve the performance and application of the proposed system.

Furthermore, the essence of an optical mouse sensor is optical flow. For an optical mouse, the lens focuses the camera onto the surface directly below the mouse and thus an optical mouse only tracks the surface directly touching or very slightly above the surface it is tracking. By interfacing an optical mouse sensor to a microcontroller and replacing the default lens with a lens focusing at a distance away, it should be possible to harness this cheap optical flow technology for many more tasks.

4.8 Conclusion

Instead of as a traditional position sensor, an optical mouse sensor can be used for non-contact tactile sensing to feel the translation direction, the height and the category of an object surface.

The angle presented on the display is not linearly related to the angle set

by the robot arm, and thus it can be seen that a-axis resolution and b-axis resolution of the optical mouse sensor are different. The characteristics of resolution vs. height can be used for height measurement and height variation of 0.2mm can be detected. Based on the feasibility of height measurement, the optical mouse sensor can be used for crack detection on a plane surface. An optical mouse sensor can feel the surface category in a non-contact way based on the characteristics of resolution vs. height of different surfaces.

There are following advantages for the optical mouse sensor. The sensor interface is ready for use. The output of the system is digital, without the need of any additional analog-to-digital component. The driver and software for the sensing system is easily available. The outputs of the sensor can be intuitively displayed on the display and recorded on the hard disk, which greatly improves the convenience of the system. Because of the large-scale manufacture of the optical mouse sensor, the sensing system is cost-effective, and thus is easily available and generalized.

In the future research, besides the non-contact tactile sensing proposed currently, based on the wavelength responsivity of an optical mouse sensor, a modified optical mouse sensor will be elementarily explored for surface color sensing. In daily life, such a home sensor can help the disabled, especially the blind. With the development of wireless technology in optical mouse sensors, such kind of application can be more flexible.

Chapter 5

Combined Tactile Sensing with Optical Mouse Sensor

5.1 Introduction

This chapter introduces the concept of multifunctional sensing and considers combined sensing as one type of multifunctional sensing. Based the idea proposed in Chapter 4, using step-by-step table-look-up method, combined tactile sensing is proposed and verified on the sandpaper.

5.2 Combined Sensing

In this chapter, *combined sensing* can be consider as one type of *multifunctional sensing*.

Depending on the functionality, the sensors can be divided into two groups, namely single function sensors and multifunctional sensors. As a

common sense, different sensors are used when there are different variables to be sensed. Different from the popular technique, known as the compound sensing, multifunctional sensors have been developed in the last decade in case the quantities being measured affect more than one single sensors input or compact structure of the sensing component is forcibly requested [40]. Employing the required number of stand-alone sensors to realize multiple functions and measure multiple measurands is the conventional sensing methodology. By a new concept, multifunctional sensors are quite different from integrated and compound sensors whereas the former one use the same structure to realize multiple functions and measure several parameters, while the latter two employs individual sensor for each function and measurement. Additionally, the multifunctional sensing can improve the sensing object discriminative property of the sensor. In most of the cases, the proposed new methodology has the following advantages over the conventional method:

1. Low cost
2. Compactness
3. Easy signal processing and interfacing

5.3 Experiment

5.3.1 Experiment Setup

The diagram of the experiment system is shown in Fig. 5.1. A robot arm of model VS-6354DM is controlled by a robot controller of model RC5-VS6A.

Both of VS-6354DM and RC5-VS6A are manufactured by DENSO Corporation. In each of X, Y and Z directions, the position repeatability of the robot arm of model VS-6354DM is $\pm 0.02\text{mm}$.

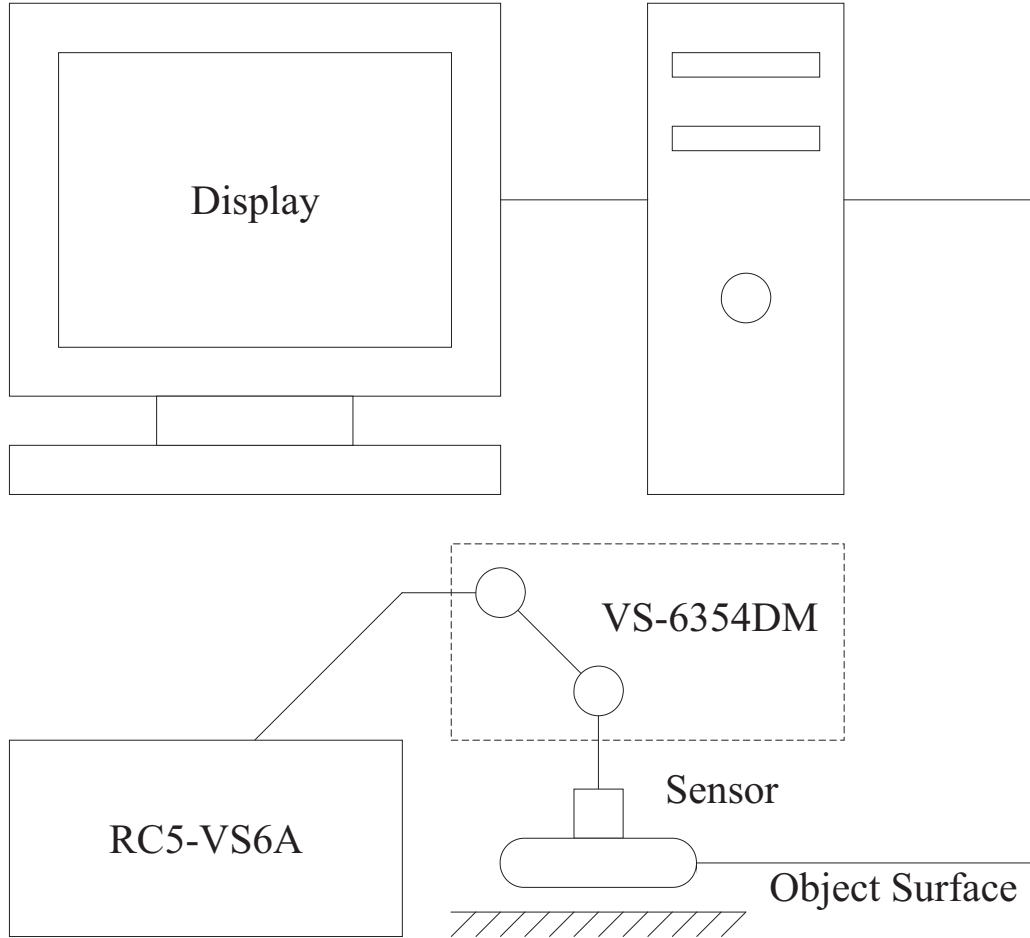


Figure 5.1: Diagram of experiment system for combined tactile sensing

The optical mouse sensor in the experiment system is from an optical mouse manufactured by Logitech, and the product number is SOM-U20. The part number of the optical mouse sensor is S2599, which is manufactured by Agilent Technologies. The nominated resolution of S2599 is 400dpi.

To ensure the isotropy of the object surfaces throughout the experiments,

sandpaper set MH913 of grit size #100, #320 and #1000 are selected as the object surfaces, which are manufactured by Musashi Holt Co., Ltd.

Throughout the experiments, in the Windows XP operating system, the pointer speed is set to the fastest and the property "Enhance pointer precision" is enabled, which help improve the system sensitivity. The resolution of the display is set as 1024×768 .

During the experiment, when the optical mouse sensor is moved over the object surface by the robot arm, the pointer position on the display varies and the pointer position is recorded by a MATLAB application.

The relative coordinate system is shown in Fig. 5.2. The $x-y$ coordinate system is the coordinate system for the object surface and the $a-b$ coordinate system is the coordinate system for the optical mouse sensor. α is the angle between a -axis and x -axis.

Fig. 5.3 shows the height from lens reference plane to object surface, denoted as z .

5.3.2 Initial Calibration

Agilent Technologies provides a computer application named "Cursor Tester" for the mouse bench test. Before the experiments, "Cursor Tester" is employed for direction calibration and parallelism calibration. The initial position and initial pose of the optical mouse sensor are adjusted by the robot arm while the outputs of "Cursor Tester" are observed and analyzed. After several recurrences of calibration, when α is 0° , if the optical mouse sensor is moved in the x -axis direction, there is zero displacement in the vertical axis

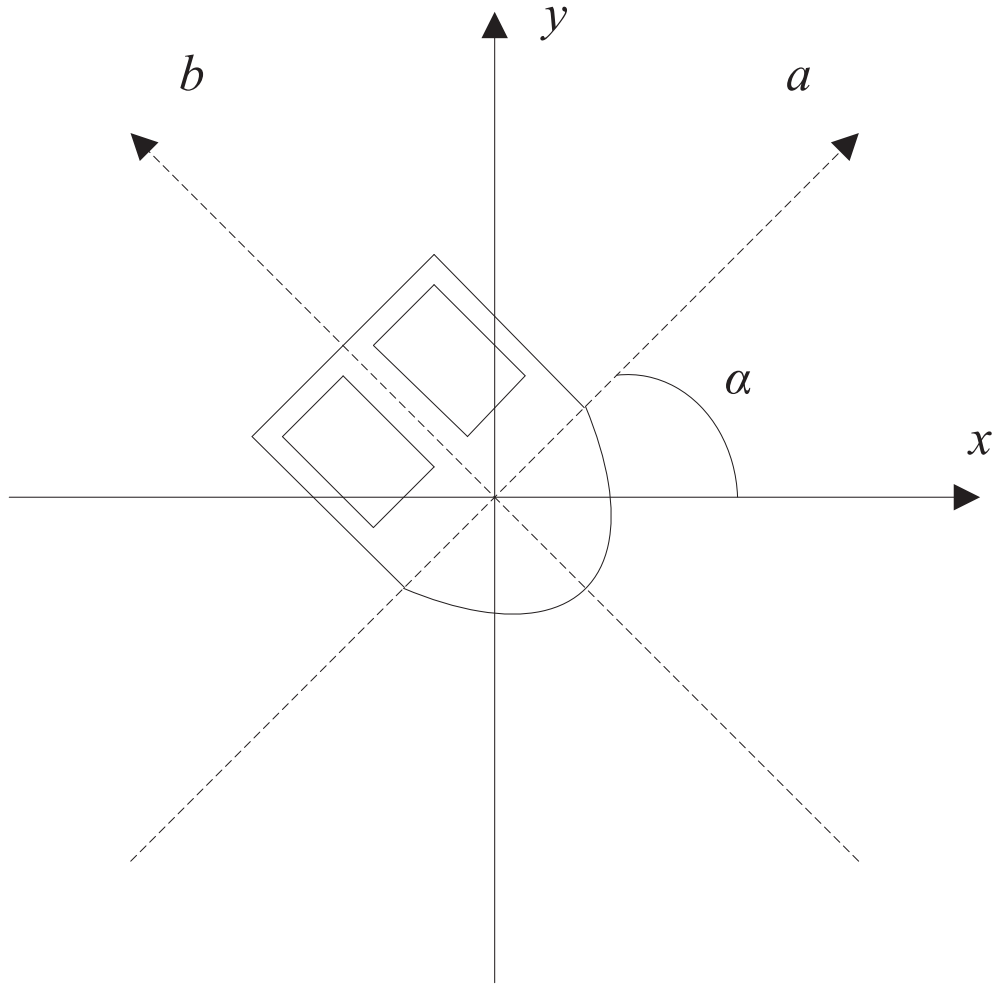


Figure 5.2: Sensing coordinate systems for the combined tactile sensing

direction on the display; if the optical mouse sensor is moved in the y -axis direction, there is zero displacement in the horizontal axis direction on the display; and the lens reference plane is parallel to the object surface.

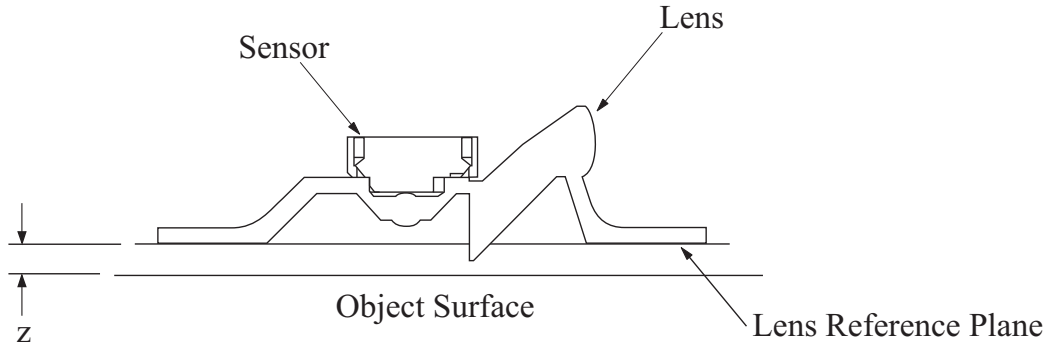


Figure 5.3: Height from lens reference plane to surface

5.3.3 Experiment Procedures

In the experiments, for a given z and a given α initially set by the robot arm, the optical mouse sensor is moved over the object surface at a uniform velocity of 1mm/s and in the y -axis direction, while the pointer position on the display varies and the pointer position is recorded by the MATLAB application.

In the MATLAB application, the sampling interval is set as 0.05s and each group of data includes 100 points, so the total sampling time for each group is 5s. The output of the sensing system is a sequence (x_i, y_i) , which describes the track of the pointer on the display. x_i is in the interval $[1, 1024]$ and y_i is in the interval $[1, 768]$. The length of the sequence is 100.

In order to simplify data processing, the starting point coordinate of each pointer track curve is translated to $(0, 0)$, because it is the relative displacement that makes sense.

For sandpaper of grit size #100, #320 and #1000 respectively, $z = [1.4, 1.6, 1.8, 2.0, 2.2, 2.4, 2.6, 2.8]$ mm, and $\alpha = [0, 10, 20, 30, 40, 50, 60, 70, 80, 90]^\circ$. Finally, 240 sequences of dimension 100×2 are obtained.

5.4 Analysis

The obtained data is organized as a table. The dimension of the data table is $3 \times 8 \times 10 \times 100 \times 2$, that is 3 surface categories, 8 surface heights, 10 surface translation directions and 100 pairs of (x_i, y_i) .

Based on the relativity of movement, the translation direction and the height of the object surface can be obtained from α and z respectively. The measurement of α is independent of z .

5.4.1 Surface Translation Direction Measurement

The 1st dimension and 2nd dimension of the data table, that is (x_i, y_i) , are employed to calculate the angle α . One estimate of $\tan(\alpha)$ is the solution in the least squares sense to the overdetermined system of equations $\mathbf{Y}_{100 \times 1} \tan(\alpha') = \mathbf{X}_{100 \times 1}$. For calculation of each $\tan(\alpha')$, the average of 24 solutions of equations corresponding to 3 surface categories and 8 values of z are used. The relation between the estimated angle α' and the actual angle α is shown in Fig. 5.4.

It can be seen that α' and α is not linearly related and a cubic polynomial provides a good fitting. That is, the angle α' presented on the display is not linearly related to the angle α set by the robot arm.

5.4.2 Surface Category Discrimination

As a human hand touches the sandpaper of different grit size, the feel is slightly different, and an optical mouse sensor can also feel the difference between the sandpapers with different grit size in a non-contact way.

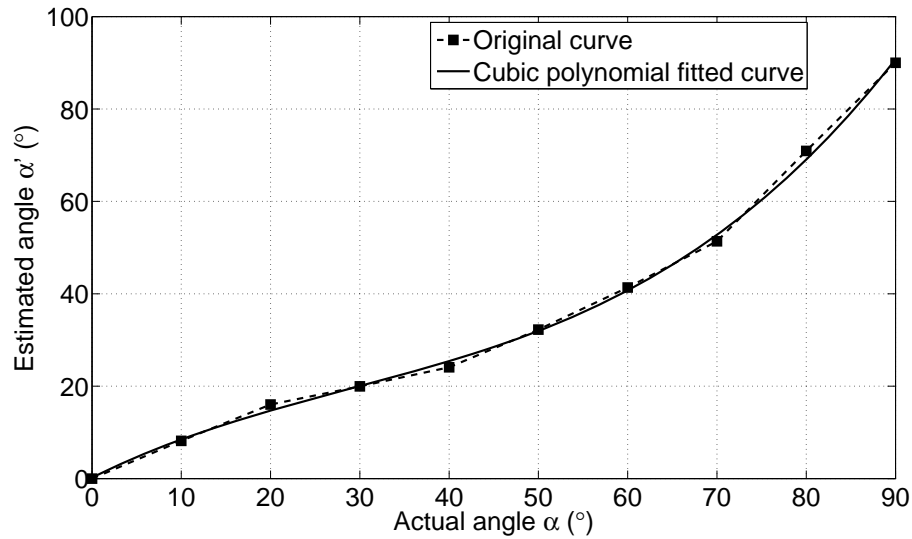


Figure 5.4: Estimated angle vs. actual angle for the surface translation direction measurement

The resolution vs. height characteristics of the 3 different surfaces are shown in Fig. 5.5. For each object surface, the characteristics of resolution vs. height are specific, and a specific characteristics curve can be recognized by a specific curve segment. In order to recognize a specific characteristics curve, another additional optical mouse sensor cooperates, with a calibrated height difference (e.g. 0.2mm) between the two optical mouse sensors.

After the translation direction measurement, for a given α (e.g. $\alpha = 0^\circ$), based on the 1st dimension, the 2nd dimension and 4th dimension of the data table, by matching the outputs of the two optical mouse sensors, a specific characteristics curve can be identified, and therefore the category of the object surface can be discriminated.

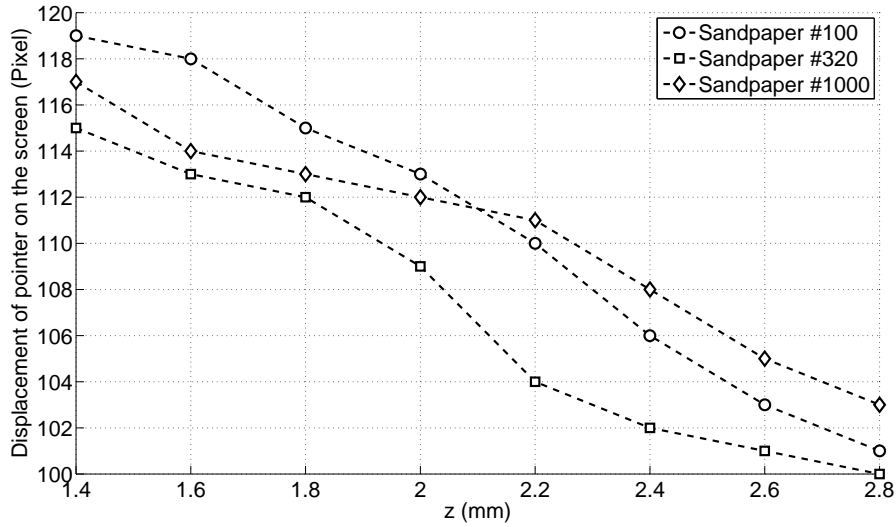


Figure 5.5: Resolution vs. height characteristics for surface category discrimination

5.4.3 Surface Height Measurement

For different object surface, the position and range of the monotonic interval of the characteristics of resolution vs. height are different. In the characteristics of resolution vs. height of an object surface, if the height variation range of the object surface is less than the range of a monotonic interval of the characteristics of resolution vs. height, by setting the initial height between the lens reference plane and the object surface properly, the height variation interval of the object surface can fall into the monotonic interval. In such a condition, the characteristics of resolution vs. height can be used for height measurement effectively. Besides, the position and range of the monotonic interval of the characteristics of resolution vs. height can also be adjusted by tuning the focus of the lens.

It can be seen that height variation of 0.2mm can be detected. For dif-

ferent object surface, the position and range of the monotonic interval of the characteristics of resolution vs. height are different.

After the surface category discrimination, for a given angle (e.g. $\alpha = 0^\circ$) and a given surface category (e.g. Sandpaper #320), the height of the optical mouse sensor can be measured, as shown in Fig. 5.6. Cubic spline provides a good fitting.

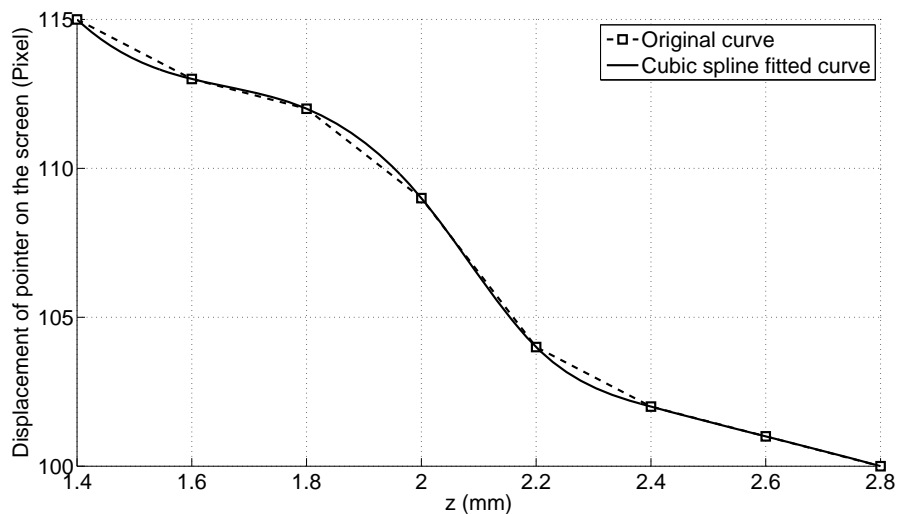


Figure 5.6: Surface height measurement in the combined tactile sensing

5.4.4 Summary

When an object surface is moved underneath the optical mouse sensor with the output of the optical mouse sensor recorded, the translation direction, the category and the height of the object surface can be obtained with a step-by-step table-look-up method based on a predefined data table, as shown in Fig. 5.7. Firstly, with a recorded pointer track and an interpolation, α can be obtained based on Fig. 5.4; secondly, with α , the displacement recorded by

the pointer track is transformed to the the displacement corresponding to a specific translation direction (e.g. $\alpha = 0^\circ$), and then the surface category can be discriminated with a double table-look-up based on Fig. 5.5; and thirdly, with the specific translation direction (e.g. $\alpha = 0^\circ$) and the surface category, z can be obtained with a table-look-up and an interpolation based on Fig. 5.6. The predefined table can be extended to help improve the combined tactile sensing.

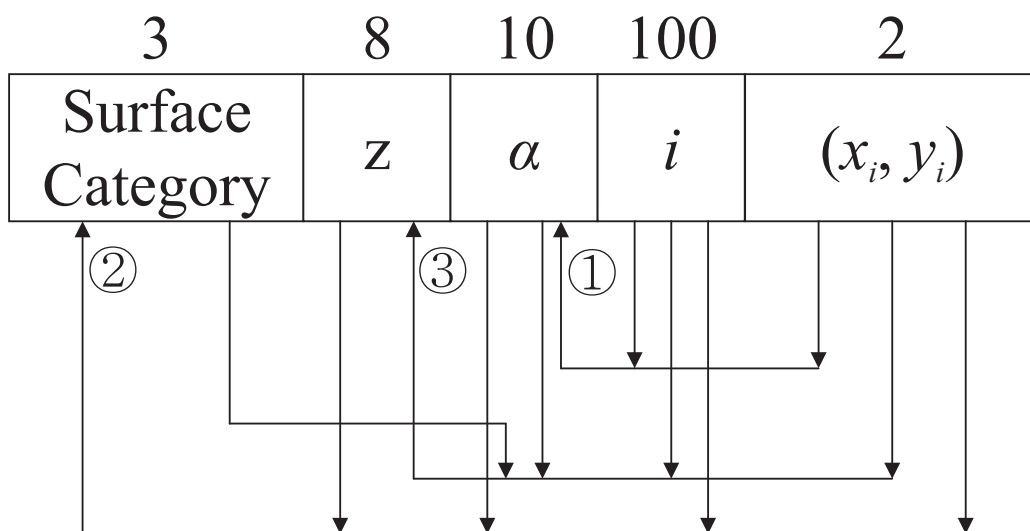


Figure 5.7: Diagram of step-by-step sensing procedures in combined tactile sensing

5.5 Discussion

The angle presented on the display is not linearly related to the angle set by the robot arm. It can be concluded that the a -axis resolution is less than the b -axis resolution. This is because the illumination of the LED is from the side, not vertically and symmetrically. The default resolution is referred to

the b -axis resolution.

In the experiments above, x is in the interval $[1, 1024]$ and y is in the interval $[1, 768]$. In actual application, there may be some cases when x and y are out of ranges above. In fact, this is a limitation caused by the driver software of the computer mouse. In actual application, the output signals of the optical mouse sensor, which is a two-channel quadrature output, can be directly used for processing. In such a way, without the intervention of the operating system and the driver software, smaller height variation can be measured and the measurement speed can be improved. Furthermore, the two-channel quadrature output can be transformed by logic circuits to be used for PWM (Pulse Width Modulation) control in some industry applications.

Besides the height from lens reference plane to object surface and the category of the object surface, many other factors, such as the velocity of the sensor, LED current level and the wavelength responsibility of the LED, influence the resolution of the optical mouse sensor and the output of the optical mouse sensor. In our current research, these parameters are constant, and the effects of them will be studied in further research work.

Furthermore, the essence of an optical mouse sensor is optical flow [14]. For an optical mouse, the lens focuses the camera onto the surface directly below the mouse and thus an optical mouse only tracks the surface directly touching or very slightly above the surface it is tracking. By interfacing an optical mouse sensor to a microcontroller and replacing the default lens with a lens focusing at a distance away, it should be possible to harness this cheap optical flow technology for many more tasks.

5.6 Conclusion

Instead of as a traditional position sensor, an optical mouse sensor can be used for combined tactile sensing to feel the translation direction, the category and the height of an object surface in a step-by-step way.

There are following advantages for the optical mouse sensor. The sensor interface is ready for use. The output of the system is digital, without the need of any additional analog-to-digital component. The driver and software for the sensing system is easily available. The outputs of the sensor can be intuitively displayed on the display and recorded on the hard disk, which greatly improves the convenience of the system. Because of the large-scale manufacture of the optical mouse sensor, the sensing system is cost-effective, and thus is easily available and generalized.

In the future research, besides the combined tactile sensing proposed currently, based on the wavelength responsivity of an optical mouse sensor, a modified optical mouse sensor will be elementarily explored for surface color sensing. In daily life, such a home sensor can help the disabled, especially the blind. With the development of wireless technology in optical mouse sensors, such kind of application can be more flexible.

Chapter 6

Conclusions and Recommendations

6.1 Introduction

The overall goal of the thesis is to apply the optical mouse sensor to the field of tactile sensing. The optical mouse sensor is used for surface shape analyzing, non-contact tactile sensing and combined tactile sensing respectively.

In Chapter 3, a device for analyzing the surface shape is reported, taking advantage of an optical mouse sensor. For smooth surface, the device can record the surface shape digitally, and for rough surface, the device can estimate the roughness in a statistical way. The resolution of the device is restricted by the resolution of the optical mouse sensor and the size of the ballpoint in the "antenna".

In Chapter 4, two series of experiments are performed on rubber surfaces and whitepaper. For the rubber surface, the periodically-square-shaped sur-

face and the periodically-arc-shaped surface can be distinguished and some shape parameters of the two object surfaces can be obtained. As a sensor working in motion, the translation direction of the object surfaces can be obtained. For the whitepaper, The translation direction, the height and the category of an object surface can be sensed.

In Chapter 5, based on the experimental characteristics of the optical mouse sensor, with a step-by-step table-look-up method, a combined tactile sensing system is proposed. When an object surface is moved underneath the optical mouse sensor, the translation direction, the category and the height of the object surface can be obtained with the recorded output of the optical mouse sensor based on a predefined data table.

6.2 Recommendations for Future Work

Besides the distance from lens reference plane to surface, many other factors, such as the velocity of the sensor, LED current level, the wavelength responsibility of the LED and the material of the object surface, influence the resolution of the optical mouse sensor and the output of the optical mouse sensor. In our current research, these parameters are constant, and the effects of them can be studied in further research work.

Besides the LED-based optical mouse sensor, the laser optical mouse sensor with superior performance is gradually popularized. The laser optical mouse sensor is enabled with Agilent's LaserStream Technology. LaserStream navigation engines provide much finer precision and more accurate tracking on a wider variety of surfaces, part of which proves difficult for

traditional LED-based optical navigation, such as glossy and reflective surfaces. The adoption of the LaserStream Technology will help improve the performance and application of the proposed system.

Currently, the optical mouse sensors have been used in the robot odometry. Not just for odometry, we expect that other useful surface configuration information can be obtained and transferred to the robot by the optical mouse sensor. In the future research, besides surface height variation sensing, based on the wavelength responsivity of an optical mouse sensor, a modified optical mouse sensor will be elementarily explored for surface color sensing. In daily life, such a home sensor can help the disabled, especially the blind. With the development of wireless technology in optical mouse sensors, such kind of application can be more flexible.

Furthermore, the essence of an optical mouse sensor is optical flow. For an optical mouse, the lens focuses the camera onto the surface directly below the mouse and thus an optical mouse only tracks the surface directly touching or very slightly above the surface it is tracking. By interfacing an optical mouse sensor to a microcontroller and replacing the default lens with a lens focusing at a distance away, it should be possible to harness this cheap optical flow technology for many more tasks.

Publications

Journal papers

1. Wang Xin and Katsunori Shida. Optical mouse sensor for non-contact tactile sensing. IEEJ Transactions on Sensors and Micromachines. Vol. 128, No. 9.
2. Wang Xin, Akira Kimoto and Katsunori Shida. Combined tactile sensing with optical mouse sensor. SICE Journal of Control, Measurement, and System Integration. Submitted.
3. Wang Xin, Akira Kimoto and Katsunori Shida. Surface shape analyzing device using optical mouse sensor. European Journal of Physics. Submitted.

International conferences

1. Wang Xin and Katsunori Shida. Optical mouse sensor for detecting height variation and translation of a surface. 2008 IEEE International Conference on Industrial Technology. 21-24 April 2008, Sichuan Uni-

versity, Chengdu, China.

Domestic conferences

1. Wang Xin, Akira Kimoto and Katsunori Shida. Optical mouse sensor for detecting height and translation of a surface. Technical Meeting on Instrumentation and Measurement, IEE Japan. Vol. IM-07, No. 29-43, pp. 7-12. 2007.
2. Wang Xin, Akira Kimoto and Katsunori Shida. Optical mouse sensor for combined tactile sensing. Technical Meeting on Instrumentation and Measurement, IEE Japan. To be presented in September 2008.
3. Wang Xin, Akira Kimoto and Katsunori Shida. Surface shape analyzing using proposed optical mouse sensor. Technical Meeting on Instrumentation and Measurement, IEE Japan. To be presented in September 2008.

Bibliography

- [1] A. F. Blackwell A. R. Jansen and K. Marriott. A tool for tracking visual attention: The restricted focus viewer. *Behavior Research Methods, Instruments, and Computers*, 35(1):57–69, 2003.
- [2] D Post B Han and P Ifju. Moire interferometry for engineering mechanics: current practices and future developments. *The Journal of Strain Analysis for Engineering Design*, 36(1):101–117, 2001.
- [3] J. Borenstein. Experimental results from internal odometry error correction with the omnimate mobile robot. *IEEE Transactions on Robotics and Automation*, 14(6):963–969, 1998.
- [4] Nadir N. Dudul Charniya and Sanjay V. Neural network based sensor for classification of material type and its surface properties. In *Proceedings of the 2007 International Joint Conference on Neural Networks*, pages 424–429, 2007.
- [5] A.J. Davison and D.W. Murray. Simultaneous localization and map-building using active vision. *IEEE Transactions on Pattern Analysis and Machine Intelligence*, 24(7):865–880, 2002.

- [6] Brenner E. and Smeets J. B. J. Fast corrections of movements with a computer mouse. *Spatial Vision*, 16(3-4):365–376, 2003.
- [7] Renshi Sawada Eiji Higurashi and Takahiro Ito. Monolithically integrated optical displacement sensor based on triangulation and optical beam deflection. *Applied Optics*, 38(9):1746–1751, 1999.
- [8] Jong-Ahn Kim Eui Won Bae and Soo Hyun Kim. Multi-degree-of-freedom displacement measurement system for milli-structures. *Measurement Science and Technology*, 12(9):1495–1502, 2001.
- [9] SEKIMORI DAISUKE MASUTANI YASUHIRO MIYAZAKI FUMIO FUJIMOTO RYOHEI, ENOMOTO MASAYA. Dead reckoning for mobile robots using optical mouse sensor. *Nippon Kikai Gakkai Robotikusu, Mekatoronikusu Koenkai Koen Ronbunshu*, 2002(Pt.1):1A1.G01(1)–1A1.G01(2), 2002.
- [10] M. Moreno J. Palacin G. Chapinal, S.S. Bota and A. Herms. A 128×128 cmos image sensor with analog memory for synchronous image capture. *IEEE Sensors Journal*, 2(2):120–127, 2002.
- [11] Merri J. Rosen Gus K. Lott and Ronald R. Hoy. An inexpensive sub-millisecond system for walking measurements of small animals based on optical computer mouse technology. *Journal of Neuroscience Methods*, 161(1):55–61, 2007.
- [12] R. N. Haward. Strain hardening of thermoplastics. *Macromolecules*, 26(22):5860–5869, 1993.

- [13] ANDO YOSHINOBU HIRAKAWA SHINGO and MIZUKAWA MAKOTO. Development of omni-directional mobile robot environment with optical mouse sensor. *Nippon Robotto Gakkai Gakujutsu Koenkai Yokoshu (CD-ROM)*, 24:3F17, 2006.
- [14] Berthold K. P. Horn and Brian G. Schunck. Determining optical flow. *Artificial Intelligence*, 19:185–203, 1981.
- [15] W. L. Xu J. Cooney and G. Bright. Visual dead-reckoning for motion control of a mecanum-wheeled mobile robot. *Mechatronics*, 14:623–637, 2004.
- [16] I. Valganon J. Palacin and R. Pernia. The optical mouse for indoor mobile robot odometry measurement. *Sensors and Actuators A*, 126:141–147, 2006.
- [17] I. Valganon J. Palacin, J. A. Salse and X. Clua. Building a mobile robot for a floor-cleaning operation in domestic environments. *IEEE Transactions on Instrumentation and Measurement*, 53(5):1418–1424, 2004.
- [18] E Kontou and P Farasoglou. Determination of the true stress-strain behaviour of polypropylene. *Journal of Materials Science*, 33(1):147–153, 1998.
- [19] Soohyun Kim Kyung-Chan Kim, Jong Ahn Kim and Yoon Keun Kwak. A robust signal processing algorithm for linear displacement measuring optical transmission sensors. *Review of Scientific Instruments*, 71(8):3220–3225, 2000.

- [20] Kok-Meng Lee and Debao Zhou. A real-time optical sensor for simultaneous measurement of three-dof motions. *IEEE/ASME Transactions on Mechatronics*, 9(3):499–507, 2004.
- [21] Shyh-Tsong Lin. Three-dimensional displacement measurement using a newly designed moir interferometer. *Optical Engineering*, 40(5):822–826, 2001.
- [22] Cornelis A. Grimbergen Magdalena K. Chmarra, Niels H. Bakker and Jenny Dankelman. Trendero, a device for tracking minimally invasive surgical instruments in training setups. *Sensors and Actuators A*, 126:328–334, 2006.
- [23] Rahkonen T. Makynen A. and Kostamovaara J. A binary photodetector array for position sensing. *Sensors and Actuators A: Physical*, 65(1):45–53, 1998.
- [24] A. Martinelli. The odometry error of a mobile robot with a synchronous drive system. *IEEE Transactions on Robotics and Automation*, 18(3):399–405, 2002.
- [25] Umberto Minoni and Andrea Signorini. Low-cost optical motion sensors: An experimental characterization. *Sensors and Actuators A*, 128:402–408, 2006.
- [26] T. W. Ng. Analysis of the optical reconstruction of shearograms using oblique illumination. *Review of Scientific Instruments*, 68(8):3125–3129, 1997.

- [27] T. W. Ng. Optical distance sensing using digital speckle shearing interferometry. *Optics and Lasers in Engineering*, 26(4-5):449–460, 1997.
- [28] T. W. Ng. The optical mouse as a two-dimensional displacement sensor. *Sensors and Actuators A*, 107:21–25, 2003.
- [29] T. W. Ng. Measuring viscoelastic deformation with an optical mouse. *Journal of Chemical Education*, 81:1628–1629, 2004.
- [30] T. W. Ng and K. T. Ang. The optical mouse for vibratory motion sensing. *Sensors and Actuators A*, 116:205–208, 2004.
- [31] T. W. Ng and K. T. Ang. The optical mouse for harmonic oscillator experimentation. *American Journal of Physics*, 73(8):793–795, 2005.
- [32] T. W. Ng and T. L. Cheong. The optical mouse as an inexpensive region-of-interest position recorder in optical microscopy. *Microscopy Research and Technique*, 63(4):203–205, 2004.
- [33] E. J. Nijhof. On-line trajectory modifications of planar, goal-directed arm movements. *Human Movement Science*, 22(1):13–36, 2003.
- [34] J. Pratt and N. B. Turk-Browne. The attentional repulsion effect in perception and action. *Experimental Brain Research*, 152(3):376–382, 2003.
- [35] Kyung-Chan Kim Se Baek Oh and Soo Hyun Kim. An averaging method for optical triangulation displacement sensors using diffraction grating. *Review of Scientific Instruments*, 72(6):2822–2826, 2001.

- [36] Daisuke Sekimori and Fumio Miyazaki. Dead-reckoning for mobile robots using multiple optical mouse sensors. *Transactions of the Society of Instrument and Control Engineers*, 41(10):775–782, 2005.
- [37] Daisuke Sekimori and Fumio Miyazaki. Self-localization for indoor mobile robots using multiple optical mouse sensor values and simple global camera information. *Transactions of the Japan Society of Mechanical Engineers. C*, 71(712):3478–3485, 2005.
- [38] T. L. Cheong T. W. Ng and J. Sheridan. Digital readout manometer using an optical mouse. *European Journal of Physics*, 28(2):N11–N16, 2007.
- [39] Noel Servagent Thierry Bosch and Silvano Donati. Optical feedback interferometry for sensing application. *Optical Engineering*, 40(1):20–27, 2001.
- [40] Chuantong Wang and Katsunori Shida. A new multifunctional space angle sensor using capacitance method. *IEEE Transactions on Sensors and Micromachines*, 126(1):1–6, 2006.
- [41] Ming Wang and Guanming Lai. Displacement measurement based on fourier transform method with external laser cavity modulation. *Review of Scientific Instruments*, 72(8):3440–3445, 2001.
- [42] Peng Zhou and Kenneth E. Goodson. Subpixel displacement and deformation gradient measurement using digital image/speckle correlation (disc). *Optical Engineering*, 40(8):1613–1620, 2001.